
# DISSERTATION

For the degree of

MSc in Human Cognitive Neuropsychology

# White matter integrity and visual short-term memory binding in familial Alzheimer's disease

Exam. no: B002317

August, 2011

**Abstract**

The asymptomatic phase of familial Alzheimer's disease caused by E280A mutation in presenilin-1 gene is characterized by intact performance in traditional neuropsychological tasks including memory, language, and executive functions. However, asymptomatic mutation carriers are already impaired in tasks that require visual short-term memory binding. Meanwhile, neuropathological changes in white matter integrity take place during the course of familial Alzheimer's disease. We investigated whether the behavioural short-term memory binding deficits are accompanied by changes in white matter integrity in asymptomatic and clinical phases of familial Alzheimer's disease.

Three groups - asymptomatic carriers of presenilin-1 gene mutation, familial Alzheimer's disease patients, and healthy controls - underwent an assessment consisting of a neuropsychological test battery, two visual short-term memory binding tasks, and diffusion tensor imaging. Group comparisons indicated changes in white matter integrity in familial Alzheimer's disease patients and to smaller extent already in asymptomatic carriers. Higher performance in visual shape-colour binding task was related to higher white matter integrity in frontal areas, and higher performance in visual colour-colour binding task was related to higher white matter integrity in frontal and parietal areas.

Thus, we demonstrate the early changes in white matter integrity already in asymptomatic phase of familial Alzheimer's disease. These changes become more widespread in the course of the disease. In addition, impaired performance in visual short-term memory binding tasks is accompanied by changes in white matter integrity which might implicate loss of connectivity. The results help to shed light on the neural underpinnings of familial Alzheimer's disease and might lead to development of new methods for the early diagnosis of Alzheimer's disease.

# Contents

# 1 Introduction

Currently, Alzheimer's disease affects an estimated 35.6 million people worldwide (Wimo & Prince, 2010). Due to the aging of the world's population, it has been predicted that by the year 2050 the worldwide prevalence of Alzheimer's will be 106.8 million (Brookmeyer, Johnson, Ziegler-Graham, & Arrighi, 2007). Early interventions can delay the disease onset and progression and can significantly decrease the global burden of the disease (Brookmeyer et al., 2007). However, reliable methods for early diagnosis of Alzheimer's disease are still under investigation.

One problem related to the investigation of the early course of Alzheimer's disease is the uncertainties related to the characteristics of the population that will develop Alzheimer's disease. A possible solution comes in the form of the more rare form, familial Alzheimer's disease, caused by gene mutations of three known genes. Carriers of these gene mutations will with almost 100% certainty develop an early-onset form of familial Alzheimer's disease with similar symptoms as the more common form, sporadic Alzheimer's disease (Goldman et al., 2011). Thus, the study of these mutation carriers can open new windows in the presymptomatic phase of Alzheimer's disease with possible new methods for early diagnosis.

In recent years, both behavioural and neuroimaging approaches to the early changes of Alzheimer's disease have proved useful (see, e.g., Saykin et al., 2010). Behaviourally, deficits in associative learning and especially short-term memory binding functions have been identified already in asymptomatic carriers of gene mutations leading to familial Alzheimer's disease (Parra, Abrahams, Logie, Mendez, et al., 2010; Parra et al., 2011). From a neuroimaging perspective, there is a search for neuroanatomical and functional changes underlying the course of Alzheimer's disease, and changes in both gray and white matter have been reported (see Frisoni et al., 2007; Bronge, Bogdanovic, & Wahlund, 2002). However, the white matter changes underlying the course of familial Alzheimer's disease remain yet sparsely studied (but see (Ringman et al., 2007)). Therefore, this study will examine changes in white matter integrity underlying the asymptomatic and clinical phases of familial Alzheimer's disease.

Also the relationship between the behavioural and brain-related changes in the course of familial Alzheimer's disease remains yet to be investigated. This study will address the question of whether the deficits in short-term memory binding can be linked to the changes in white matter integrity in familial Alzheimer's disease due to the mutation E280A of the Presenilin-1 gene (see Lopera et al., 1997).

# 2 Diffusion tensor imaging

## 2.1 The study of white matter integrity

The properties of the brain white matter can be studied with several structural brain imaging methods. Tradionally, magnetic resonance imaging (MRI) has proved useful in detecting macroscopic changes in brain tissue including tissue loss (atrophy). However, macroscopic changes in brain tissue take place usually only at the final stage of neuropathological diseases and therefore are not useful in clinical practise including the distinction between different forms of neuropathological diseases such as dementias (Bozzali & Cherubini, 2007). However, macroscopic changes are usually preceded by microstructural changes in the brain tissue (Bozzali & Cherubini, 2007). Thus, methods for studying these microstructural changes are needed in order to fully understand the underlying pathophysiological processes leading to macroscopic changes.

A possible solution for studying the microstructural changes in brain white matter comes in the form of diffusion tensor imaging (DTI), a method that relies on the principles of MRI and knowledge of the mobility of water molecules (diffusion). DTI uses diffusion-weighted MR signals that are made sensitive to diffusion by using a specific magnetic field gradient pulse sequence (see Stejskal & Tanner, 1965) and can be used to produce maps of microscopic displacements of water molecules in the tissue which then reveal details about the architecture of the tissue (Le Bihan, 2003). In brain tissue, cell membranes, fibres and macromolecules block the free displacement of the water molecules causing the molecules to move freely only to certain directions (Le Bihan, 2003). Therefore, detecting the displacement of the water molecules with DTI provides information on tissue composition, the physical properties of tissue constitutes, tissue microstructure and its architectural organization (Basser & Jones, 2002).

Particularly in brain white matter, water diffusion is not equal in all directions but greater in one direction than another (Gulani & Sundgren, 2006). This high anisotropy of white matter is well-established and results roughly from the organization of white matter tissue as bundles of myelinated axonal fibres running in parallel (Le Bihan, 2003). However, the exact mechanism of diffusion anisotropy is yet not well understood (Beaulieu, 2002).

The white matter bundles in healthy tissue are highly structured and aligned in a distinct direction, but pathological processes related to some diseases may modify the white matter integrity and leave a signature to the diffusion properties that can be detected with DTI (Horsfield & Jones, 2002; Bozzali & Cherubini, 2007). Disruptions of diffusivity related to pathological processes in the spinal cord and brain white matter were first measured with DTI in the end of the 1980s in cats and humans (Moseley et al., 1990; Chenevert, Brunberg, & Pipe, 1990).To date, the clinical value of DTI has been shown in conditions such as white matter diseases (leukoaraiosis, MS, ALS), brain ischemia and injuries, HIV, and brain tumors (see Horsfield & Jones, 2002, for a review), and

increasingly also neurodegenerative diseases including dementias (for a review, see Bozzali & Cherubini, 2007).

Next, the key concepts related to DTI are briefly introduced followed by examples on how DTI and behavioural measures have been combined.

## 2.2 A brief introduction to DTI principles

Diffusion imaging (DI) was first used in 1985 (Taylor & Bushell, 1985; Merboldt, Hanicke, & Frahm, 1985; Le Bihan & Breton, 1985) DI used a single apparent diffusion coefficient (ADC) estimated for each voxel from a series of diffusion- weighted images using linear regression. However, a single coefficient was insufficient for measuring the diffusivity in anisotropic substances such as white matter since information about molecular displacement was available only in one direction (see Basser, 1995). Therefore, diffusion tensor imaging (DTI, Basser, Mattiello, & LeBihan, 1994; for reviews see Le Bihan et al., 2001; Basser, 1995; Mori & Barker, 1999) was developed to expand diffusion imaging to three-dimensional space. Instead of a single coefficient, DTI uses a diffusion tensor which is a symmetrical matrix

$$\mathrm{D} = \begin{bmatrix} D_{xx} & D_{yx} & D_{zx} \\ D_{xy} & D_{yy} & D_{zy} \\ D_{xz} & D_{yz} & D_{zz} \end{bmatrix} \tag{1}$$

The diffusion tensor D is an array of several coefficients that fully describes molecular mobility along each direction and correlation between these directions and is estimated in each voxel. Thus, DTI provides a more accurate estimate of diffusivity in an anisotropic medium.

Diffusion data acquired with DTI can be analysed in three ways using parameters that are derived from the diffusion tensor (Le Bihan, 2003). First, mean diffusivity ($\bar{D}$) characterizes the overall mean-squared displacement of molecules and the overall presence of obstacles to diffusion and reflects the overall water content of the medium (Le Bihan et al., 2001; Le Bihan, 2003). Mean diffusivity is defined as

$$\bar{D} = (D_{xx} + D_{yy} + D_{zz})/3, \tag{2}$$

where $D_{xx}$, $D_{yy}$, $D_{zz}$ are the mean-squared displacements of molecules in each direction (see Basser, 1995). Histopathological studies suggest that increased mean diffusivity most likely results from the loss of neurons, axons, and dendrites (Bronge et al., 2002).

Second, anisotropy indices can be used to indicate how anisotropic the diffusion is (Pierpaoli & Basser, 1996), that is, to describe the degree to which molecular displacements vary in space (Le Bihan et al., 2001; Le Bihan, 2003). The degree of anisotropy is related to the

presence and coherence of orientated structures (Le Bihan et al., 2001; Le Bihan, 2003). Fractional anisotropy (FA) is one of the most commonly used invariant anisotropy indices and it is defined as

$$\mathrm{FA} = \sqrt{3[(\lambda_1 - \langle\lambda\rangle)^2 + (\lambda_2 - \langle\lambda\rangle)^2 + (\lambda_3 - \langle\lambda\rangle)^2]} / \sqrt{2(\lambda_1^2 + \lambda_2^2 + \lambda_3^2}, \quad (3)$$

where $\lambda_1$, $\lambda_2$, $\lambda_3$ are the eigenvalues of the diffusion tensor D, and $\langle\lambda\rangle = (\lambda_1 + \lambda_2 + \lambda_3)/3$ (Basser, 1997). FA measures the fraction of the magnitude of mean diffusivity that can be ascribed to anisotropic diffusion, ranging from isotropic diffusion (0) to infinite anisotropy (1). Anisotropy indices might reflect myelin fiber integrity (Le Bihan, 2003) which is supported by the finding that the anisotropy index of white matter increases during brain development possibly due to the process of myelination (see, e.g., Sakuma et al., 1991; Wimberger et al., 1995). Furthermore, reduced FA most likely results from a change in tissue cytoarchitecture due to subtle small vessel alterations, demyelination of axonal structures, and possibly gliosis (Brun & Englund, 1986; Bronge et al., 2002).

Third, main direction of diffusivities is linked to the structure orientation in the space (Le Bihan, 2003) and is usually described by using colour-coded maps. In this study, only mean diffusivity ($\bar{D}$) and fractional anisotropy (FA) measures are used.

After the acquisition of diffusion tensor data, the data has to be quantified for the investigation of white matter abnormalities. The methods for data quantification are briefly introduced next.

## 2.3 DTI data quantification

The first and probably the most extensively used quantification method is the *regions of interest* (ROI) approach where preselected ROI(s) are placed manually or semi-automatically on FA maps of each participant separately from which DTI indices can then be calculated and compared across participants (Park et al., 2003). ROI based methods are especially useful when previous knowledge guides the selections of ROI or with patients populations with large variability in brain anatomy. However, ROI approach requires subjective decisions on placement especially in regions that are difficult to distinguish from individual images (Smith et al., 2006), making results inconsistent across studies due to possible differences in definitions of anatomical borders of regions (Baron et al., 2001; Busatto et al., 2003). Also, ROI methods are time-consuming and labor-intensive (Busatto et al., 2003). Furthermore, ROI approach limits the study to prespecified regions leaving other potentially important regions undetected (Good et al., 2001). With these limitations in mind, ROI methods can still provide useful quantification of DTI data.

Other methods have been suggested to solve some of the problems of ROI methods. First, *voxel-based morphometry* (VBM) analyses can be used to detect potential changes in brain tissue in the whole brain without the need to preselect regions of interest (Ashburner

& Friston, 2000, Smith et al. 2006). In general, using VBM first requires the spatial normalization of all the images to the same template image, then extracting different brain tissue types (gray matter, white matter and cerebrospinal fluid) from the normalized images followed by smoothing, and finally performing a voxelwise statistical analysis to locate group differences or task covariants (Ashburner & Friston, 2000). VBM method is fully automated and simple to apply (Smith et al., 2006), and extends the analysis from selected regions of interest to comprehensive assessment of anatomical differences throughout the brain (Ashburner & Friston, 2000). Especially, VBM can be used in an exploratory way in studies where the ROI of potential abnormality is difficult to define (Park et al., 2003). However, VBM suffers from problems caused by variabilities and inaccuracies in the results of spatial normalization, and effects of smoothing to the final results (Bookstein, 2001; Park et al., 2003, Smith et al. 2006). For instance, more careful examinations have revealed that apparent changes in DTI indices shown with VBM might be related to anatomical differences such as changes in ventricle size (Simon et al., 2005).

Second, tractography-based approaches can overcome the alignment and smoothing problems of VBM (Smith et al., 2006). In tractography-based methods, seeds for start and target ROIs are defined and fiber bundle tracking is performed to track the white matter tracts between these two points (see Conturo et al., 1999; Behrens et al., 2003). For instance, tractography has been useful in detecting longitudinal white matter changes in the whole tract, and not just in its parts as ROI approach would require (Davis et al., 2009). However, only the tracts that can be reliably traced and separated from other tracts can be used for the analysis which limits the potential regions included in the analysis (Smith et al., 2006). Also, similarly to ROI based methods, a problem of objectivity and accuracy arises when the start- and end-seeds of tracts are identified by user, and trajectories are especially sensitive for the placement of seed point (S. Smith et al., 2006; Tench, Morgan, Wilson, & Blumhardt, 2002).

Third, *tract-based spatial statistics* (TBSS, Smith et al. 2006, 2007) method was developed to bring together the strengths of tractograpy-based and VBM approaches. Indeed, TBSS should overcome the alignment and smoothing problems or VBM (Smith et al., 2006). In TBSS, a common registration target is identified to which all subjects' FA images are aligned. Then, a mean of all aligned images is created and thinned to create a mean skeleton, after which each subject's aligned FA image is projected to the skeleton.Finally, voxelwise statistics are performed across subjects on the skeleton-space FA data. TBSS is fully automated and investigates the whole brain (Smith et al., 2006). However, it is possible that pathology can reduce FA so strongly that potential areas of interest may be wrongly excluded from analysis due to the thresholding of the mean FA values on the skeleton (Smith et al., 2006).

In recent years, also the amount of studies combining DTI indices with behavioural measures has increased, with applications to different cognitive domains including memory, executive functions and language (e.g., Burgmans et al., 2011; Ystad et al., 2011; Charl-

ton, Barrick, Lawes, Markus, & Morris, 2010; de Zubicaray, Rose, & McMahon, 2011; Ryan et al., 2008; Frye et al., 2010; Loui, Li, & Schlaug, 2011; Madden et al., 2004), and to clinical populations including schizophrenia (Nestor et al., 2004), Alzheimer's disease (see, e.g., (Chen et al., 2009)), traumatic brain injury (Kraus et al., 2007), and aphasia (Meinzer et al., 2010). VBM and TBSS allow the voxelwise statistics to be calculated between each voxel and behavioural measure directly (Frye et al., 2010; Loui et al., 2011; Scholz, Klein, Behrens, & Johansen-Berg, 2009). In ROI approaches, DTI indices are first calculated for each regions of interest and various methods can then be used to examine the relationship between the DTI indices from each ROI and behavioural variables.

# 3 Neuroanatomy of Alzheimer's disease (AD)

## 3.1 Characterization of familial AD

Alzheimer's disease (AD) is the most common form of dementia accounting for about 50 to 70 % of the late-onset cases of dementia (Querfurth & LaFerla, 2010). AD is characterized clinically by progressive loss of memory and pathologically by the presence of large numbers of neuritic plaques and neurofibrillary tangles.

Clinically, the earliest sign of AD is a subtle decline in memory functions followed by worsened mental cababilities and personality changes. Later on, language functions and visuospatial performance is impaired. At the final stage of the disease, also motor system is affected. (Small et al. 1997)

The neuropathological diagnosis of AD requires the presence of abnormal alteration in intraneuronal cell structure (Braak et al., 1999). The two main pathological features of AD include the extracellular deposition of beta-amyloid-containing plaques (Small & McLean, 1999) and the alterations in intraneuronal cell structure which eventually take the form of neurofibrillary tangles and neuropil threads (Braak & Braak, 1991; Braak et al., 1999). The neurofibrillary changes evolve in different stages from transentorhinal regions to hippocampal formation and entorhinal regions, and from there to adjoining higher order association areas of the neocortex, and finally to other areas of neocortex (Braak & Braak., 1991). Typically, the diagnosis is made only when the neurofibrillary changes have already expanded to neocortical areas (Braak et al., 1999). Of neocortical areas, especially temporoparietal regions are generally affected in AD (see Horsfield & Jones, 2002).

The principal risk factor for AD is age, but otherwise the etiology of AD is under continuous research. Especially, genetic risk factor underlying AD have been vigorously researched in the recent years (see Avramopoulos, 2009). The only gene proved to increase the risk for the more common late-onset sporadic form of AD (SAD) is the APOE $\epsilon 4$ allele (Strittmatter et al., 1993; Saunders et al., 1993, see also Bertram & Tanzi, 2008; Avramopoulos, 2009). In relation to the other form, the early-onset familial form of Alzheimer's disease (FAD), mutations in three different genes have been identified to lead to the disease (see, e.g., Goldman et al., 2011). These genes include the amyloid precursor protein (APP) gene in chromosome 21 (Goate et al., 1991), presenilin-1 gene on chromosome 14 (Sherrington et al., 1995), and presenilin-2 gene on chromosome 1 (Levy-Lahad et al., 1995), all of which alter the APP processing (Hardy, 1997). Mutations in these three genes lead to FAD that is clinically and neuropathologically similar to SAD but has an early onset before the age of 60 to 65 years of age (but see Holmes, 2002). Several different mutations can affect these three genes (see, e.g., Clark et al., 1995). For instance, one mutation that has been extensively researched is the E280A single mutation of the presenilin-1 gene which causes a form of AD that is clinically identical to the range

of signs and symptoms seen in SAD (Lopera et al., 1997; Ardila et al., 2000). The E280A mutation leads to FAD in 100 % of the cases with the average onset time of 47 years of age (Lopera et al., 1997).

Although the principal pathological changes in both SAD and FAD have been reported mainly in the grey matter (see Horsfield & Jones, 2002), also white matter changes take place. Post-mortem examinations have revealed white matter changes in AD resulting mainly from partial loss of axons, myelin sheaths, and oligodencroglial cells and from other intraneuronal processes (Brun & Englund, 1986). These changes were found most prominently in frontal lobes, central regions, and parietal lobes but expanded to the whole brain white matter in the course of the disease (Brun & Englund, 1986). With DTI, the study of white-matter integrity in human *in vivo* has also become possible. The DTI results on the disruption of white matter in AD will be discussed next.

## 3.2 Changes in white matter integrity in AD

To our knowledge, there has been only study to the date using DTI to examine the white matter integrity changes in FAD mutation carriers. Ringman et al. (2007) compared the FA values in selected brain areas (fornix, cingulum, perforant pathway, genu and splenium, frontal white matter and corticospinal tract) for 15 presymptomatic FAD subjects of which 8 were presenilin-1 or APP mutation carriers and 7 non-carriers serving as controls. Mutation carriers were found to have reduced FA in two areas: in the fornix and left frontal white matter anterior and superior to the orbitofrontal cortex.

Another possibility to study preclinical AD is to investigate the white matter changes in carriers of the APOE $\epsilon 4$ allele, a mutation that is a known risk factor for developing SAD. It has been shown that the fractional anisotropy of carriers of at least one copy of APOE $\epsilon 4$ allele is reduced in splenium of corpus callosum, occipito-frontal fasciculus, and hippocampus (Persson et al., 2006).

White matter changes in preclinical and presymptomatic SAD have been widely studied using individuals with mild cognitive impairment (MCI) who have a higher risk of developing dementia (see Petersen, 2004). Although the possible pre-SAD effects seen in MCI patients cannot be directly compared to presymptomatic FAD, DTI studies with MCI patients can reveal brain areas that might be important also in presymptomatic FAD. However, the white matter changes related to MCI are inconsistent across different studies. While some studies have found no changes in fractional anisotropy in MCI patients compared to healthy controls in the areas under investigation (Damoiseaux et al., 2009; Fellgiebel et al., 2004; Mielke et al., 2009; Pievani et al., 2010), other studies have reported increased fractional anisotropy of MCI patients in projection fibers including posterior cingulum, anterior and posterior thalamic radiations, thalamic peduncles and even fornix (Kiuchi et al., 2009; Medina et al., 2006; Zhang et al., 2007; Zhuang et al., 2010), association fibers including superior and inferior longitudinal fasciculi, and inferior

fronto-occipital fasciculus (Medina et al., 2006; Zhuang et al., 2010), general white matter areas that include different types of fibers such as centrum semiovale and frontal, temporal, parietal and occipital white matter (Douaud et al., 2011; Zhuang et al., 2010; Medina et al., 2006), and white matter underlying the medial temporal lobes including parahippocampal white matter (Rose et al., 2006; Zhang et al., 2007). Also, some studies have reported no differences in mean diffusivity between MCI patients and controls (Medina et al., 2006; Pievani et al., 2010), other studies have shown decreased mean diffusivity of MCI patients in hippocampal areas and posterior cingulum (Kiuchi et al., 2009; Zhang et al., 2007; Fellgiebel et al., 2004; Kantarci et al., 2005), and in centrum semiovale and temporal white matter (Fellgiebel et al., 2004).

Taken together, results regarding white matter integrity especially from the studies with MCI patients are rather ambiguous. The disparities in results between different studies might be due to sample composition (e.g., different types or stages of MCI), or methods used for data analysis (e.g., ROI selection, ROI vs. whole-brain methods) (see Damoiseaux et al., 2009; Medina et al., 2006). Furthermore, since results from MCI or SAD studies are not directly comparable with FAD, more research is needed using FAD population to understand the processes underlying this form of AD.

# 4 Short-term memory binding

## 4.1 What is short-term memory binding?

The world consists of complex objects and episodes that are characterized by their components: features of a single entity such as shape, colour or movement, or several entities that are temporarily combined. Thus, a mechanism is needed to bind the information relating to each object or episode (Treisman, 1996). In the framework of long-term memory, this is usually called associative memory referring to the mechanism for storing associations. In short-term memory, the term binding is often used (Vogel, Woodman, & Luck, 2001; Zimmer, Mecklinger, & Lindenberger, 2006).

Binding appears in several forms with probably different underlying mechanisms (see Figure 1). At the first level, there is a distinction between intra-item and inter-item associations (see, e.g., Piekema, Rijpkema, Fernández, Kessels, & Aleman, 2010). Intra-item associations are associations between objects and their features that can be bound together and perceived as a single entity . Intra-item associations can be further divided to two subtypes, namely intrinsic and extrinsic object features referring to features that are either an aspect of the item itself (within-item feature, e.g., colour) or defined by the spatiotemporal characteristics of the event, respectively (e.g., current context) (see, e.g., Ecker, Zimmer, & Groh-Bordin, 2007; Kahneman, Treisman, & Gibbs, 1992). Inter-item associations are formed by separate items and are not perceived or remembered as one entity (Mayes, Montaldi, & Migo, 2007). Inter-item associations can be further divided to within-domain associations and between-domain associations (Mayes et al., 2007; Piekema et al., 2010). Within-domain associations are formed between similar types of items or features (e.g. face-face associations) and are likely to be represented by activity in same or closely interacting neocortical structures (Mayes et al., 2007). Between-domain associations are formed between different types of items (e.g. face-word associations) processed in anatomically separate structures and may require a distinct neural structure for their integration (Mayes et al., 2007).

Also other concepts of binding exists such as crossmodal binding or distinctions between unimodal and polymodal associations (see, e.g., (Karlsen, Allen, Baddeley, & Hitch, 2010; Lavenex & Amaral, 2000), but the focus in the current study will be in intra-item binding.

## 4.2 Neural correlates of binding

In the context of long-term memory (LTM), associative memory has been linked to medial temporal lobes (see Lavenex & Amaral, 2000; Mayes et al., 2007). Associations from temporal, frontal and parietal lobes project to parahippocampal and perirhinal areas in medial temporal lobes where multimodal information is integrated, from there to the

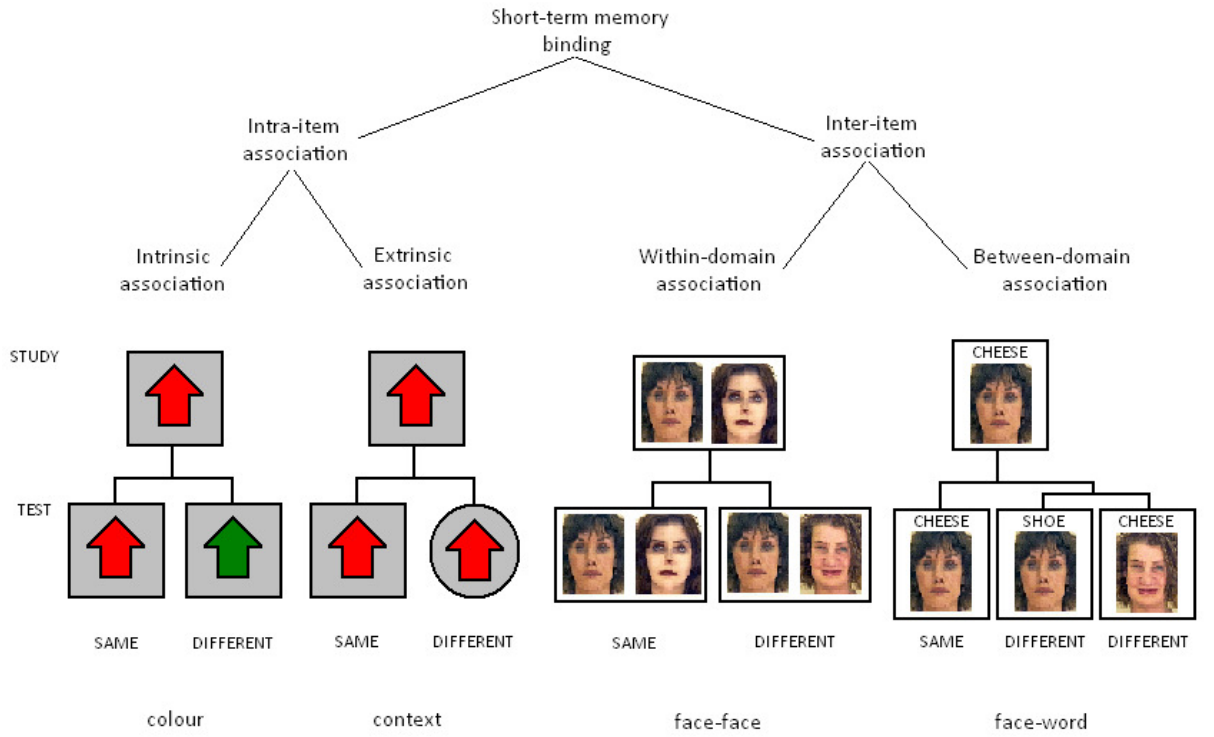


Figure 1: Different forms of binding. Below the subtypes, an example of a task used to study each form of binding is presented. See text for details. (Intra-item association examples based on Ecker et al., 2007, inter-item examples on Mayes et al., 2007. Face images adapted from Psychological Images Collection at Stirling (PICS), pics.stir.ac.uk.)

entorhinal cortex, and finally to hippocampal formation with increasing abstract hierarchy along the way. Furthermore, hippocampal formation then returns the higher-order representations to be stored in neocortex.

However, it seems that visual short-term memory (STM) associations are not necessarily dependent on medial temporal lobes. Studies in patients with damage to medial temporal lobes have demonstrated preserved abilities in visual STM binding (Jeneson, Mauldin, & Squire, 2010; Baddeley, Allen, & Vargha-Khadem, 2010). Yet, neuroimaging studies have shown that medial temporal lobes might be important in some aspects of binding. For instance, within-domain encoding seems to activate areas of hippocampus, parietal lobe and prefrontal cortex, whereas recognition might be related to activation only in prefrontal and parietal areas (Achim & Lepage, 2005). Furthermore, Piekema, Kessels, Mars, Petersson, and Fernández (2006) and Piekema et al. (2010) showed that hippocampus might be active during the maintenance of integrated spatial and identity information, but not during maintenance of feature only or integrated colour and identity information.

Therefore, other areas might contribute more to visual STM binding. Especially, the importance of prefrontal cortex including especially the right middle and superior frontal gyri and left inferior frontal gyri has been demonstrated in several visual STM binding tasks (Prabhakaran, Narayanan, Zhao, & Gabrieli, 2000; Sala & Courtney, 2007; Achim & Lepage, 2005; Uncapher, Otten, & Rugg, 2006; Piekema et al., 2010). Also, parietal

cortex seems to play a role in extrinsic intra-item binding including colour and location (Uncapher et al., 2006; Piekema et al., 2010). For the part of intrinsic intra-item binding including for instance colour and object information, it is possible that the information is integrated already in higher-order visual processing stages (van Essen, Anderson, & Felleman, 1992).

Taken together, the most promising areas for visual STM binding include areas in prefrontal cortex and parietal lobes. Thus, binding does not take place in a single brain area but possibly depends on a network of several connected brain areas.

## 4.3 Binding deficits in AD

Traditionally, cued recall paired-associate learning (PAL, e.g. Wechsler, 1945) tasks have been used to differentiate AD from other kinds of dementias and healthy aging. In PAL tasks, participants are usually presented with increasingly large sets of different items that combine multiple features (e.g., object and location, two words). After the presentation of the whole set, the memory for individual items is tested using cued recall, that is, one feature is presented and the corresponding other feature has to be recalled.

AD patients have shown to be impaired in different PAL tasks including pattern-location, face-name, visuospatial and verbal associations (Gallo, Sullivan, Daffner, Schacter, & Budson, 2004; Pariente et al., 2005; Sperling et al., 2003). Moreover, AD has been shown to be differentiable from other diseases with partially similar clinical features including frontotemporal dementia and semantic dementia (Lee, Rahman, Hodges, Sahakian, & Graham, 2003) and depression (Swainson et al., 2000). Also, PAL tasks can detect AD already in the preclinical phase of the disease (Lindeboom, Schmand, Tulner, Walstra, & Jonker, 2002). However, the use of PAL in the early diagnosis suffers from the finding that also healthy ageing is related to impairments in task performance (e.g., De Jager, Milwain, & Budge, 2002).

The relationship between AD and PAL task performance seems to stem from medial temporal lobe dysfunction in AD (see Lowndes & Savage, 2007): since especially hippocampus is important for associative learning, the sensitivity of PAL task to AD has been linked to early damage to hippocampus (Mayes et al., 2007; Lowndes et al., 2008). The relationship between medial temporal lobes and PAL task performance also suggests that PAL task relies on associative memory in LTM.

Another line of research focuses on STM binding deficits in AD. STM binding tasks generally use a change-detection paradigm where shortly after the presentation of a sample array, the participants are presented with a test array and have to indicate whether the two arrays were identical or different in terms of either a single feature or a combination of features (Luck & Vogel, 1997; Vogel et al., 2001). Thus, while some trials test for memory of single features alone, the completion of the other trials requires successful encoding and retrieval of bound features.

Using this STM binding task, patients with SAD have been found to be impaired in both verbal (Parra et al., 2009) and visual (Parra et al., 2011) STM tasks. Also, visual STM binding functions are impaired in early-onset FAD caused by E280A mutation of presenilin-1 gene already in the asymptomatic phase of the disease (Parra, Abrahams, Logie, Mendez, et al., 2010; Parra et al., 2011). Interestingly, unlike PAL task the visual STM binding performance is not affected by age (Brockmole, Parra, Sala, & Logie, 2008). Also, visual STM binding task can distinguish between SAD and depression (Parra, Abrahams, Logie, & Della Sala, 2010). This sensitivity of visual STM binding to AD makes it a potential tool for detecting early AD.

The tasks that have been used so far in AD literature test either intrinsic or extrinsic intra-item associations. For instance, the shape-colour binding task (e.g., Parra, Abrahams, Logie, Mendez, et al., 2010; Parra et al., 2011) requires the binding a shape and its colour and, thus, represents intrinsic intra-item binding. In another task that has been used, namely the colour-colour binding task (Parra et al., 2011), background colour has to be bound to shape colour, thus representing extrinsic intra-item binding where the colour of the background frame forms a context for the colour of the shape.

However, the neural underpinnings of STM binding deficits in AD remain unclear. STM binding does not seem to require hippocampus (e.g., Piekema et al., 2010), but might depend on the effective connections between different brain areas. Thus, it is possible that visual STM binding deficits in AD result from changes in connectivity rather than neural loss such as hippocampal atrophy (see, e.g., Parra, Abrahams, Logie, Mendez, et al., 2010).

Taken together, associative LTM learning tasks have been shown to be sensitive to AD but are also affected by age. The relationship between AD and these tasks probably stems from medial temporal lobe dysfunction in AD which is the first neuropathological marker of the disease. On the other hand, STM binding tasks provide a method for detecting early AD without interfering age-related effects. However, since STM binding tasks do not rely on medial temporal lobes, the deficits in these tasks might stem on processes other than neural loss in medial temporal lobes and reflect processes that remain yet to be identified.

# 5 Aims and hypotheses

In summary, FAD is characterized by both behavioural and neuroanatomical markers, but the nature of these changes and their relation to each other remains yet unclear. Thus, the first aim of this study is to expand the knowledge of changes in white matter integrity related to FAD. To date, there has been only one study investigating the changes in white matter integrity in FAD (Ringman et al., 2007), and this study used a rather small dataset comparing only presymptomatic mutation carriers and non-carriers. The current study will aim for more generalisability by including both asymptomatic mutation carriers and FAD patients. Also, Ringman et al. concentrated on fractional anisotropy only; however, changes in mean diffusivity might be a more sensitive indicator for white matter changes in AD (Fellgiebel et al., 2004; Bozzali et al., 2002). In this study, we expand the investigation to cover mean diffusivity as well.

The second aim of this study is to investigate how the changes in white matter integrity in FAD are related to changes in behavioural performance. There is a growing interest in combining DTI and behavioural information, but no studies have concentrated on asymptomatic mutation carriers of FAD. Specifically, we ask whether the STM binding deficits observed in FAD can be accounted for by a loss of the white matter integrity.

It is hypothesized that changes in white matter integrity are observed in FAD patients and to some extent also in asymptomatic carriers of the mutation. Also, we hypothesize that lower binding scores are related to a loss of white matter integrity in regions affected by AD such as frontal, temporal, and parietal lobes as well as their connecting tracts. Furthermore, it is hypothesized that changes in white matter integrity across the selected ROIs will differentially account for poor performance in STM binding tasks than in paired-associative (PAL) tasks.

# 6 Methods

## 6.1 Participants

The participants are a subset of a sample previously reported in Parra, Abrahams, Logie, Mendez, et al. (2010) and Parra et al. (2011, Experiment 2). All the participants are members of a large kindred from the Colombian province of Antioquia, South America. The members of this kindred carry a gene mutation E280A of presenilin-1, presence of which leads in 100 % of cases to an autosomic dominant familial Alzheimer's disease which becomes clinically detectable at on average 47 years of age (see Lopera et al., 1997 for a clinical description of the disease).

The recruitment protocol for all the participants consisted of three phases. First, genetic screening was performed to confirm the presence of the mutation using the methodology reported by the Alzheimer's Disease Collaborative Group (Clark et al., 1995, see also Lemere et al., 1996; Lendon et al., 1997). Second, once the genotype was confirmed, the neurological and neuropsychological assessments were performed by individuals who were blind to the genetic condition of the participants. Based on these assessments, participants were classified in three groups: 1) participants with early-onset familial Alzheimer's disease caused by the E280A single presenilin-1 mutation (FAD patients), 2) carriers of the mutation who did not meet Alzheimer's disease criteria (asymptomatic carriers), and 3) healthy individuals who were not carriers of the gene mutation and who were relatives of the members of the other two groups (healthy controls). Third, DTI data was acquired from a subset of the participants.

The final sample consisted of 58 participants in three groups. The demographic characteristics of the groups are presented in Table 1. First, FAD patients groups includes 19 participants diagnosed according to the criteria established by the Diagnostic and Statistical Manual of Mental Disorders (4th edition, text revision) and the National Institute of Neurological and Communicative Disorders and Stroke and the Alzheimer's Disease and Related Disorders Association (NINCDS-ADRDA) group (McKhann et al., 1984).

Second, asymptotic carriers group consisted of 18 participants who met neither Alzheimer's disease nor mild cognitive impairment criteria (Petersen, 2004) at the time of the testing but who were positive for the E280A mutation.

Third, healthy controls group included 21 non-carriers who were relatives of the FAD carriers and asymptomatic carriers. Additional inclusion criteria for the control participants included 1) negative history of neurological or psychiatric disorders, 2) Mini-Mental State Examination (MMSE) score equal or greater than 24, and 3) no memory complaints as documented by a self-report and a family questionnaire.

Asymptomatic carriers and healthy controls were matched according to age, the number of years spent in formal education, and the MMSE scores (see Table 1). On average,

FAD patients were older and less educated than the two other groups. However, previous studies have shown that education and age do not affect the performance in visual STM binding tasks (Brockmole et al., 2008; Parra et al., 2011).

Each participant underwent a colour vision assessment using the Dvorine pseudo-isochromatic plates (Dvorine, 1963) and a binding perception condition. These assessments were undertaken to rule out the possibility that poor performance on the STM binding task could result from visual or perceptual difficulties. None of the participants recruited for the present study were excluded due to colour vision or perceptual binding problems.

All participants gave informed consent to take part in the study which was approved by the Ethics Committee at University of Antioquia, Colombia.

Table 1: Demographic data for the participants.

| | FAD ($n$ = 19) | AC ($n$ = 18) | HC ($n$ = 21) | One-way ANOVA | | | |
|---|---|---|---|---|---|---|---|
| | | | | | Post-hoc $t$ tests ($p$) | | |
| | Mean (sd) (Range) | Mean (sd) (Range) | Mean (sd) (Range) | $F(df = 2)$ | FAD vs HC | AC vs HC | FAD vs AC |
| Age | 47.5 (6.4) (38-66) | 35.1 (5.5) (24-43) | 39.3 (8.3) (25-54) | 15.46, $p < .001$ | .001 | n.s. | <.001 |
| Education | 7.3 (3.7) (2-14) | 10.2 (3.9) (2-16) | 10.3 (2.7) (4-13) | 4.50, $p < .05$ | .024 | n.s. | .038 |
| MMSE Score | 23.6 (4.3) (17-30) | 29.8 (0.4) (29-30) | 29.6 (0.7) (28-30) | 39.41, $p < .001$ | <.001 | n.s. | <.001 |

FAD = FAD patients, AC = asymptomatic carriers, HC = healthy controls

## 6.2 Behavioural tests

### 6.2.1 Neuropsychological battery

The neuropsychological battery comprised of the Mini-Mental State Examination (Folstein, Folstein, & McHugh, 1975), the Spanish version of the Paired Associates Learning Task (Wechsler, 1945), the Spanish versions of Verbal Fluency Tests (Letter-FAS, adapted from Sumerall, Timmons, James, Ewing, & Oehlert, 1997, and Animal Fluency, from Morris, Heyman, Mohs, Hughes, et al., 1989), the Copy and Recall of the Complex Figure of Rey-Osterrieth (Osterrieth, 1944; Rey, 1941), Part-A of the Trail Making Test (Reitan, 1958), Boston Naming test (Kaplan, Goodglass, & Weintraub, 1983), the Wisconsin Card Sorting Test (Berg, 1948), and word list test (from Morris et al., 1989).

### 6.2.2 Visual short-term memory tasks

Two visual short-term memory (vSTM) tasks similar to those reported in Parra, Abrahams, Logie, Mendez, et al. (2010); Parra et al. (2011) were administered to the par-

ticipants. The tasks assessed visual STM for arrays of stimuli presented on a computer screen, and required the binding of either shape and colour, or colour and colour.

During both tasks, the memory load of the task was manipulated to match the general group performance by presenting asymptomatic carriers and healthy controls with arrays of three items and FAD patients with arrays of two items. Previous studies have shown that manipulating the memory loads allows performance levels in the baseline memory condition to be equated across groups and, thus, any differences between groups in vSTM binding performance cannot be attributed to the baseline differences in memory for single features (see, e.g., Logie, Cocchini, Delia Sala, & Baddeley, 2004; Logie, Della Sala, MacPherson, & Cooper, 2007).

The vSTM tasks used a change detection paradigm (Luck & Vogel, 1997) where participants first viewed a stimulus array presented in random position on a 15 in. PC screen using a 3 x 3 virtual grid ('study phase') and, after a short delay, were presented with test stimuli and were required to orally respond whether the test stimulus was 'same' or 'different' as the one presented in the study phase ('test phase'). The experimenter entered participants' responses using the keyboard. Three experimental conditions were used in each task. In both tasks, each condition consisted of 15 practice trials followed by 32 test trials leading to a total of 96 test trials per task. Trials were fully randomized across participants and conditions were delivered in a counter-balanced order.

In the shape-colour binding task, the stimuli were random polygon shapes (see Figure 2 a), colours, or combinations of shapes and colours. Stimuli were randomly selected from a set of eight shapes and a set of eight colours and presented either independently (vSTM for single features) or combined (vSTM binding). Each type of stimulus was presented in a separate condition. Two conditions assessed vSTM for single features and one the binding of these features in vSTM (see Figure 2 b). In the 'shape only' and 'colour only' conditions, arrays of shapes or colours were presented in the study display. In the test display for the 'different' trials, two new shapes or new colours from the study array were replaced with two new shapes or two new colours. Hence, in these conditions, only vSTM for individual features was required to detect a change. In the shape-colour binding condition, combinations of shapes and colours were presented in the study display. In the test display for 'different' trials, two shapes swapped the colours in which they had been shown in the study display. Hence, memory for bindings of shape and colour in the study display was required in order to detect this change. No shape or colour was repeated within a given array. 50% of the test trials were 'same' trials (the study and test displays presented identical items) and 50% were 'different' trials. Trials began with a fixation screen shown for 500 ms. This was followed by the study display presented for 2000 ms. After the study display, there was an unfilled retention interval of 900 ms followed by the test display.

In the colour-colour binding task, the stimuli were constructed using six different layouts, each defined by a shape and frame area (see Parra, Abrahams, Logie et al. 2009). The

(a)

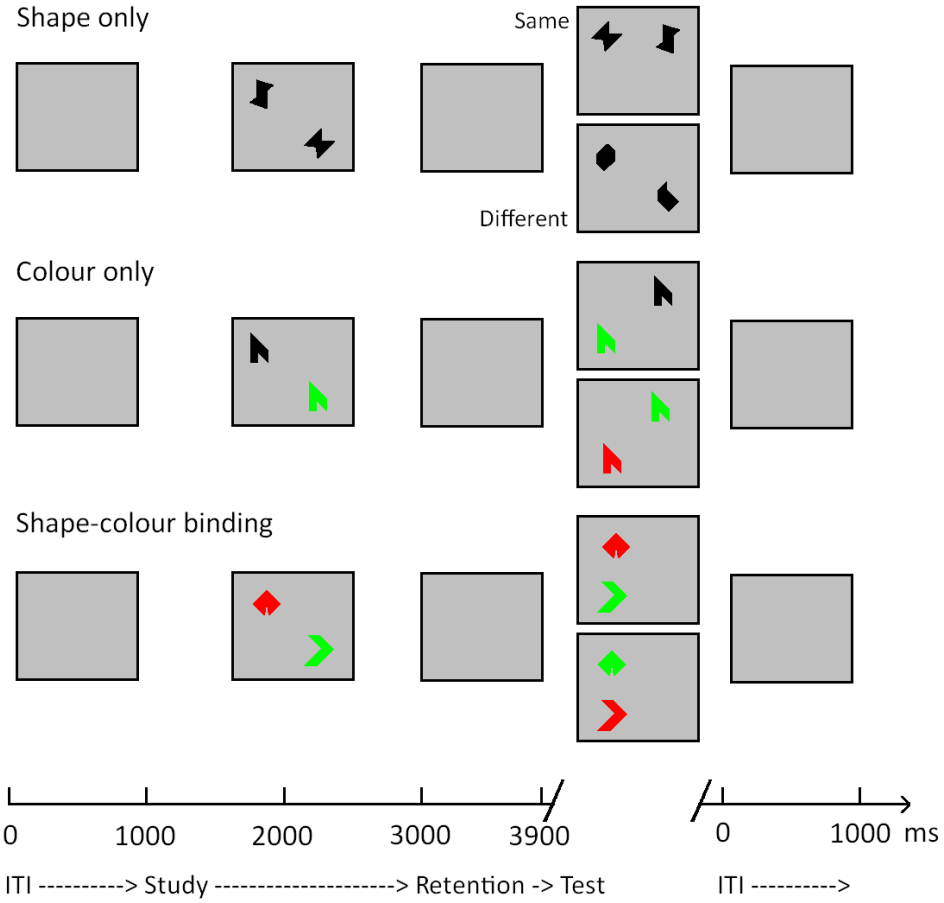


(b)

Figure 2: Shape-colour binding task. (a) Shapes used as stimuli. (b) The three conditions used in the task.

shape or frame area of each object, each representing 50% or the surface, was filled with a colour. The procedures used to select the colours and the psychophysical features of the colours selected were reported in Parra, Abrahams, Logie et al. (2009). Three experimental conditions were used (see Figure 3). In the 'colour only' condition the shape area displayed a different single colour for each object while the frame was black for all. In the 'different' trials the shape colour of two objects was replaced by a new colour which was not presented at study. In the 'unbound colours' condition both the shape and frame area of each object were shown in different colours. In the 'different' trials one colour from either the shape (50%) or the frame (50%) area in two of the objects was replaced by a new colour that had not appeared in the study display. Participants were told to focus on colours and not on their associations as the change would consist of new colours. In the condition assessing memory for 'bound colours' both the shape and frame area were of different colours. In the 'different' trials two objects swapped one colour either from

the shape (50%) or from the frame area (50%). Participants were told that colours and their associations were both relevant as sometimes colours would be rearraged in different combinations during the test display. In less than 30% of the trials, colours were repeated within a display no more than twice. This occurred in the 'unbound' and 'bound' colours conditions for controls and only in the 'unbound' colours condition for FAD patients to avoid undermining the need for binding when only two items were presented. This manipulation was aimed at increasing participants' awareness of the need to attend to all the features and to all the combinations. Trials began with a fixation cross shown for 250 ms. This was followed by a study display for 200 ms. After an unfilled retention interval of 900 ms, the test display was presented until the participant responded. There was then a gap of 1000 ms until the next trial. In half of the trials objects on both displays were the same, in the other half two of the objects in the test display showed different colours from those in the study display. Participants were requested to detect whether the study and test displays consisted of the 'same' or 'different' items and to respond orally accordingly.

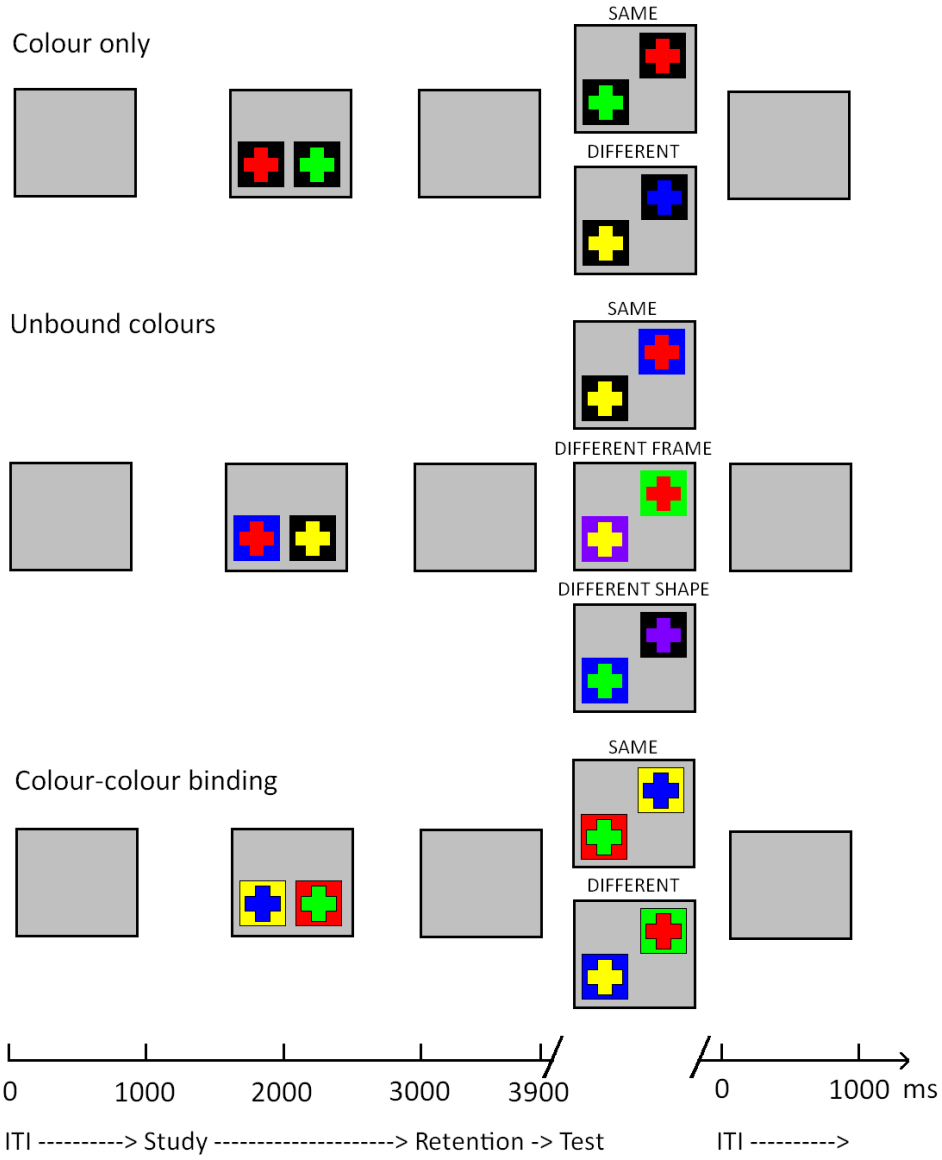


Figure 3: Colour-colour binding task. The three conditions used in the task.

In both tasks, each condition consisted of 15 practice trials followed by 32 test trials leading to a total of 96 test trials per task.

## 6.3 Diffusion tensor imaging

### 6.3.1 DTI and MRI data collection and preprocessing

Diffusion tensor MRI (DT-MRI) data were collected using a Siemens Symphony Vision 1.5 T (Siemens Healthcare Sector, Erlangen, Germany) clinical scanner, and consisted of one T2-weighted and sets of diffusion-weighted (b = 1000 s/mm2) single-shot, spin-echo, echo-planar (EP) volumes acquired with diffusion gradients applied in 12 non-collinear directions. Fifty contiguous slice locations were imaged with a field-of-view of 220 × 220 mm, an acquisition matrix of 128 × 128 and a slice thickness of 3 mm, giving an acquisition voxel dimension of 1.72 × 1.72 × 3 mm. The repetition and echo times for each EP volume were 7.2 s and 90 ms.

The DICOM format (http://medical.nema.org/) magnitude images were converted into NIfTI-1 format (http://nifti.nimh.nih.gov). Using tools freely available in FSL (FMRIB, Oxford, UK; http://www.fmrib.ox.ac.uk), the DT-MRI data were pre-processed to extract the brain, and bulk patient motion and eddy current induced artefacts removed by registering the diffusion-weighted to the T2-weighted EP volume for each subject (Jenkinson & Smith, 2001). From these MRI data, mean diffusivity ($\overline{D}$) and fractional anisotropy (FA) volumes were generated for every subject using DTIFIT.

### 6.3.2 ROI selection

The aim of the DTI analysis was to identify which regions are affected in the course of FAD and which regions might be related to the binding deficits in this population. Thus, a set of regions of interest (ROIs) in white matter was chosen among brain areas that potentially are affected in early FAD. Due to the limited previous research with DTI in FAD, also regions that are known to be affected in early course of SAD were used. In addition, regions with potential importance for binding and connections between these areas were chosen for the analysis. The criteria for selection of each ROI are summarised in Table 2.

The resulting set of consistent of 18 ROIs. The selected association fibers included the superior longitudinal fasciculus (SLF, reciprocal connections between frontal, parietal, temporal and occipital lobes), inferior longitudinal fasciculus (ILF, reciprocal connections between occipital and temporal lobes), inferior fronto-occipital fasciculus (IFO, reciprocal connections between frontal and occipital lobes), and uncinate fasciculus (UNC, reciprocal connections between anterior temporal lobes and orbital cortex). Other association fibers

Table 2: Selection of regions of interest.

| Area | Criteria for selection | References |
|---|---|---|
| **Prefrontal cortex** | | |
| dorsolateral prefrontal cortex (DL-PFC) | right area activation in visual STM binding tasks, explains individual differences in visual STM task | Prabhakaran et al. (2000); Todd and Marois (2005) |
| anterior prefrontal cortex (A-PFC) | right area activation in visual STM binding tasks | Prabhakaran et al. (2000) |
| Broca's area (BR-PFC) | left area activation in visual STM binding tasks | Uncapher et al. (2006) |
| **Association fibers** | | |
| superior longitudinal fasciculus (SLF) | reduced FA in SAD and MCI | Rose et al. (2006); Medina et al. (2006) |
| inferior fronto-occipital fasciculus (IFO) | reduced FA in APOE e4 allele carriers | Persson et al. (2006) |
| inferior longitudinal fasciculus (ILF) | reduced FA in SAD | Stricker et al. (2009) |
| uncinate fasciculus (UNC) | reduced FA in SAD | Kiuchi et al. (2009) |
| cingulum (CGC, CGH) | reduced FA in SAD and MCI, increased $\overline{D}$ in SAD, trend to reduced FA related to presymptomatic FAD | Medina et al. (2006); Salat et al. (2010); Rose et al. (2000); Ringman et al. (2007) |
| fornix (FX) | reduced FA related to presymptomatic and preclinical FAD | Ringman et al. (2007) |
| **Projection fibers** | | |
| anterior thalamic radiations (ATR) | reduced FA in MCI | Zhuang et al. (2010) |
| corticospinal tract (CST) | reduced FA in MCI and SAD, inconsistent results | Zhuang et al. (2010); Mielke et al. (2009) |
| **Corpus callosum** | | |
| genu (GCC) | age-related effects (not specific to SAD) | Head et al. (2004) |
| splenium (SCC) | reduced FA and increased $\overline{D}$ related to SAD and APOE e4 allele but not to MCI, FA and MMSE positively correlated, $\overline{D}$ and MMSE negatively correlated | Duan et al. (2006); Rose et al. (2000); Salat et al. (2010); Zhang et al. (2007); Persson et al. (2006) |
| **Lobar white matter areas** | | |
| centrum semiovale (CS) | increased $\overline{D}$ in SAD and MCI | Fellgiebel et al. (2004) |
| frontal white matter (F-WM) | increased $\overline{D}$ in MCI and SAD, FA and MMSE scores positively correlated, reduced FA in presymptomatic FAD | Bozzali et al. (2002); Bartzokis et al. (2003); Duan et al. (2006); Medina et al. (2006); Ringman et al. (2007) |
| parietal white matter (P-WM) | reduced FA and increased $\overline{D}$ in SAD, FA and MMSE scores positively correlated; superior parietal lobe activation during extrinsic intra-item binding | Bozzali et al. (2002); Fellgiebel et al. (2004); Duan et al. (2006); Head et al. (2004); Rose, Janke PhD, and Chalk (2008); Salat et al. (2010); Piekema et al. (2010) |
| temporal white matter (T-WM) | reduced FA in SAD, increased $\overline{D}$ in SAD and MCI, FA and MMSE scores positively correlated, part of ventral stream (possible importance for visual binding) | Bozzali et al. (2002); Duan et al. (2006); Fellgiebel et al. (2004); Head et al. (2004); Salat et al. (2010) |

connecting the cortex and medial temporal lobes included the hippocampal and cingulate gyrus parts of the cingulum (CGH and CGC, afferent connections from cingulate gyrus to entorhinal cortex), and the column of fornix (FX, reciprocal connections between hip-

pocampus and septal area and hypothalamus). The selected projection fibers included the anterior thalamic radiations that run through the anterior limb of the internal capsule (ATR, reciprocal connections between frontal lobe and thalamus) and the corticospinal tract in the middle portion of cerebral peduncle (CST, afferent connections from motor areas to brain stem and spinal cord). Of the callosal areas the genu (GCC, connecting anterior hemipheres) and the splenium (SCC, connecting posterior hemispheres) of corpus callosum were included. Lobar white matter areas included the centrum semiovale (CS, cerebral white matter including several association and projection fibers), frontal white matter (F-WM), parietal white matter (P-WM) and temporal white matter (T-WM). Also, subregions of prefrontal cortex were examined further using the white matter underlying the dorsolateral prefrontal cortex (DL-PFC, BA9/46 in middle frontal gyrus), anterior prefrontal cortex (A-PFC, BA10 in most anterior prefrontal cortex), and Broca's area and the corresponding area in the right hemisphere (BR-PFC, BA44/45 in inferior frontal gyrus).

### 6.3.3 ROI placement and acquisition of DTI indices

Region-of-interest (ROI) analysis was performed using 'in house' software written in MATLAB (The MathWorks, Natick, MA, USA), that allowed small square ROIs to be placed either by hand on the T2-weighted volumes and then overlaid on the co-registered $\overline{D}$ and FA maps, or automatically using locations defined in Montreal Neurological Institute (MNI; http://www.bic.mni.mcgill.ca/) standard space and transferred back to the subject's native space. In the latter, the software allows the user to interactively move ROIs if standard to native space registration errors cause white matter ROIs to be placed over cerebrospinal fluid (CSF) or grey matter structures.

The procedure for obtaining the FA and $\bar{D}$ values for each ROI is presented in Figure 4. First, MNI coordinates were defined in standard space for each ROI separately using ICBM-DTI-81 white matter atlas (Oishi, Faria, Zijl, & Mori, 2011) and then selected in the FSLview 3.1.8 from the FSL software (FMRIB, Oxford, UK; http://www.fmrib.ox.ac.uk). Typically, between 6 and 12 square boxes were defined for each ROI in horizontal view, sizes of which varied from 2x2x1 voxels to 3x3x1 voxels (see Table 3). Several boxes were used for each ROI in order to reduce the effects of differences in individual placement for the FA and $\overline{D}$ values. For MNI coordinates, see Appendix B.

The further analysis steps were performed with an in-house script in MATLAB 7.8.0. For each ROI, the coordinates were mapped from standard space to individual T2 images by using an inverse of the transformation matrix from native to standard space. The placement of the ROIs in individual images was then checked manually by using the T2-weighted images and the following criteria of no overlap with either CSF or gray matter. T2-weighted images were used instead of the FA images since it has been recommended that ROIs should be drawn on images whose contrast is independent of the quantity

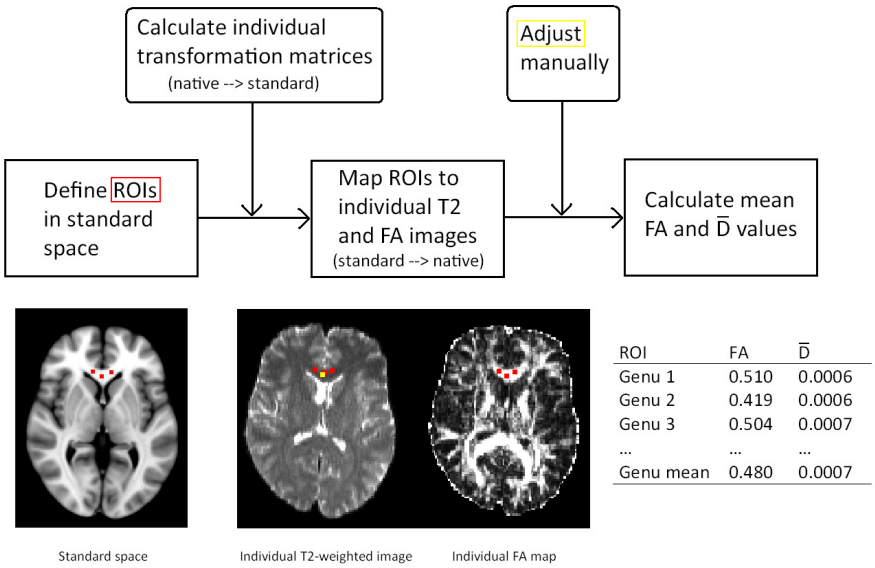


Figure 4: Procedure for ROI placement.

under analyses to avoid biasing the placement (see Bozzali & Cherubini, 2007). Manual adjustments were performed by an investigator blind to subjects' genetic or clinical status. Finally, the values for FA and $\overline{D}$ were obtained for each box and then averaged between the boxes for each ROI separately.

Table 3: Regions of interest.

| ROI | Box size (voxels) | No. of boxes | Total size (voxels) | Total size ($mm^3$) | Placement |
|---|---|---|---|---|---|
| DL-PFC | $3 \times 3 \times 1$ | 3 per side | 54 | 478.56 | 3 consecutive slices |
| A-PFC | $3 \times 3 \times 1$ | 3 per side | 54 | 478.56 | 3 consecutive slices |
| BR-PFC | $3 \times 3 \times 1$ | 3 per side | 54 | 478.56 | 3 consecutive slices |
| SLF | $3 \times 3 \times 1$ | 3 per side | 54 | 478.56 | 1 slice |
| IFO | $3 \times 3 \times 1$ | 3 per side | 54 | 478.56 | 2 consecutive slices |
| ILF | $3 \times 3 \times 1$ | 3 per side | 54 | 478.56 | 1 slice |
| UNC | $3 \times 3 \times 1$ | 3 per side | 54 | 478.56 | 3 consecutive slices |
| CGH | $3 \times 3 \times 1$ | 3 per side | 54 | 478.56 | 3 consecutive slices |
| CGC | $3 \times 3 \times 1$ | 3 per side | 54 | 478.56 | 3 consecutive slices * |
| FX | $2 \times 2 \times 1$ | 1 in middle | 4 | 35.45 | 1 slice * |
| ATR | $3 \times 3 \times 1$ | 4 per side | 72 | 638.09 | 2 consecutive slices |
| CST | $3 \times 3 \times 1$ | 3 per side | 54 | 478.56 | 3 consecutive slices |
| GCC | $3 \times 3 \times 1$ | 2 per side, 1 in middle | 54 | 478.56 | 2 slices |
| SCC | $3 \times 3 \times 1$ | 2 per side, 1 in middle | 54 | 478.56 | 2 slices |
| CS | $3 \times 3 \times 1$ | 6 per side | 108 | 957.13 | 1 slice |
| F-WM | $3 \times 3 \times 1$ | 6 per side | 108 | 957.13 | 2 slices |
| P-WM | $3 \times 3 \times 1$ | 6 per side | 108 | 957.13 | 2 slices |
| T-WM | $3 \times 3 \times 1$ | 6 per side | 108 | 957.13 | 3 consecutive slices |

* = manual placement

## 6.4 Statistical analyses

All the statistical analyses were performed in R version 2.11.1 (R Development Core Team). Statistical analyses for the behavioural variables were conducted with ANOVA and post-hoc comparisons with Tukey's test. Correlations between behavioural variables separately in each group were examined using Pearson's correlation coefficient. Hemispheric differences in FA and $\overline{D}$ values were examined with $t$ tests.

Differences in FA and $\overline{D}$ indices between groups for each ROI were examined with linear regression. Three different models were created, model fit was compared with $F$ test, and the best model was chosen according to the criteria of best model fit and most parsimony. The models tested for either a group effect alone ($\mathrm{ROI}_r^D \sim \mathrm{group}$), group and age main effects ($\mathrm{ROI}_r^D \sim \mathrm{age} + \mathrm{group}$), or group and age main effects and interaction effects ($\mathrm{ROI}_r^D \sim \mathrm{age} + \mathrm{group} + \mathrm{age} \times \mathrm{group}$). Thus, it was possible to test whether groups differed from each other even after controlling for age differences, and whether possible age differences were similar between groups. Group differences between FAD patients and controls, and asymptomatic carriers and controls could be interpreted from linear regression models directly, but to test for significant differences between FAD patients and asymptomatic carriers an *ad hoc* simulation of 1,000 repeats was run with *sim()* function from *arm* package (Gelman, Su, Yajima, & Hill, 2011).

Finally, linear regression was used to identify the ROIs with DTI indices that are related to performance in different behavioural tasks. To examine the group effects and DTI index effects in the behavioural tasks, multiple linear regression models were tested separately for each behavioural task. First, a base model was built with group as the only predictor of task score

$$\mathrm{task}_k \sim \mathrm{group}$$

where $k$ = behavioural tasks. The variable group was coded as a factor with control group serving as the baseline comparison which allowed testing for the separate effects of the membership of either FAD patient or asymptomatic carrier group. Next, age and education were separately added to the model as predictors to test for the possible age and education effects on the task. Different models were compared to each other using $F$ test and the best model was chosen according to the criteria of best model fit and parsimony. The best model was then saved as the base model. Next, two models for each ROI and for FA and $\overline{D}$ indices separately were built on top of the base model. The first model (additive model) included only the main effect of the individual ROI DTI index

$$\mathrm{task}_k \sim \mathrm{group} + \mathrm{ROI}_{r,d}$$

where $r$ = ROIs and $d$ = FA, $\overline{D}$. The second model (interaction model) included also the

interaction between groups and ROI DTI index

$$\text{task}_k \sim \text{group} + \text{ROI}_{r,d} + (\text{group} \times \text{ROI}_{r,d})$$

These models were first compared with $F$ test to the base model to see whether the ROI DTI index had any effect on the task. If both additive and interaction models had significantly better fit than the base model, they were compared to each other using $F$ test and the model with the best fit was chosen as the final model. Due to the relatively small sample size, multiple comparisons were not corrected for explicitly.

# 7 Results

## 7.1 Behavioural results

Results from group comparisons of behavioural variabels are presented in Table 4 and Table 5. FAD patients performed significantly worse than healthy controls in all neuropsychological and visual STM binding tasks except for the WCST attempts to category and Letter fluency task. FAD patients performed significantly worse than the asymptomatic carriers in all tasks except for the WCST attempts to category task and the colour-colour binding task. Asymptomatic carriers performed significantly worse than healthy controls in shape-colour binding condition, in unbound-colours condition, and in colour-colour binding condition. Correlations between behavioural variables are presented in Supplementary results (Appendix C).

Table 4: Group comparisons of visual short-term memory tasks.

| | FAD ($n = 19$) | AC ($n = 18$) | HC ($n = 21$) | One-way ANOVA | | | |
|---|---|---|---|---|---|---|---|
| | | | | | Post-hoc $t$ tests ($p$) | | |
| | Mean (sd) (Range) | Mean (sd) (Range) | 93.1 (8.1) | $F(df = 2)$ | FAD vs HC | AC vs HC | FAD vs AC |
| Shape only | 67.6 (11.6) (50-91) | 88.8 (8.4) (72-100) | 93.1 (8.1) (69-100) | 34.83, $p < .001$ | <.001 | n.s. | <.001 |
| Colour only (1) | 80.3 (17.7) (50-100) | 96.1 (5.8) (78-100) | 98.9 (1.8) (94-100) | 17.03, $p < .001$ | <.001 | n.s. | <.001 |
| Shape-colour binding | 58.7 (11.7) (47-78) | 71.8 (10.6) (56-91) | 84.1 (12.1) (59-97) | 19.20, $p < .001$ | <.001 | .004 | .009 |
| Colour only (2) | 83.0 (12.7) (59-97) | 92.5 (7.5) (75-100) | 98.0 (2.6) (91-100) | 14.41, $p < .001$ | <.001 | n.s. | .005 |
| Unbound colours | 67.1 (9.2) (53-81) | 80.7 (6.6) (69-94) | 92.1 (5.5) (75-100) | 49.30, $p < .001$ | <.001 | <.001 | <.001 |
| Bound colours | 59.2 (10.3) (44-78) | 69.2 (11.9) (41-84) | 81.5 (12.0) (56-97) | 14.90, $p < .001$ | <.001 | .005 | n.s. |

FAD = FAD patients, AC = asymptomatic carriers, HC = healthy controls

Colour only (1) = colour only condition in shape-colour binding task

Colour only (2) = colour only condition in colour-colour binding task

## 7.2 DTI indices

Comparisons between FA and $\bar{D}$ values from corresponding ROIs in left and right hemispheres revealed hemispheric differences in all regions either in FA values, $\overline{D}$ values, or both (see Appendix C). Therefore, all the following analyses were conducted for hemispheres separately.

Table 5: Group comparisons of neuropsychological tests.

| | FAD ($n = 19$) | AC ($n = 18$) | HC ($n = 21$) | One-way ANOVA | | | |
|---|---|---|---|---|---|---|---|
| | | | | | Post-hoc $t$ tests ($p$) | | |
| | Mean (sd) (Range) | Mean (sd) (Range) | Mean (sd) (Range) | $F(df = 2)$ | FAD vs HC | AC vs HC | FAD vs AC |
| PAL | 7.2 (3.2) (3-14) | 13.7 (4.1) (7-20) | 14.2 (3.0) (7-20) | 21.02, $p < .001$ | <.001 | .907 | <.001 |
| Rey copy | 17.1 (10.1) (1-29) | 27.3 (5.8) (13-36) | 26.8 (5.5) (10-34) | 11.5, $p < .001$ | <.001 | .973 | .020 |
| Rey recall | 3.0 (4.1) (0-18) | 17.1 (6.1) (8-27) | 16.4 (6.8) (2-31) | 34.3, $p < .001$ | <.001 | .914 | .000 |
| Letter fluency | 8.5 (4.2) (2-16) | 12.8 (6.3) (6-29) | 10.9 (3.3) (5-17) | 3.91, $p < .05$ | .260 | .400 | <.001 |
| Animal fluency | 13.4 (5.4) (4-26) | 21.0 (5.4) (14-32) | 19.8 (5.5) (12-31) | 10.38, $p < .001$ | .002 | .758 | <.001 |
| Boston naming | 11.7 (1.6) (8-15) | 13.7 (1.3) (11-15) | 13.6 (1.3) (10-15) | 12.71, $p < .001$ | <.001 | .962 | <.001 |
| Word list immediate | 10.6 (5.8) (3-22) | 20.4 (4.0) (11-26) | 19.3 (3.5) (11-27) | 26.9, $p < .001$ | <.001 | .747 | <.001 |
| Word list delayed | 2.0 (2.6) (0-8) | 7.3 (1.6) (4-10) | 7.6 (1.3) (5-10) | 52.03, $p < .001$ | <.001 | .904 | <.001 |
| Word list recognition | 15.2 (3.2) (9-20) | 19.6 (0.7) (18-20) | 19.6 (0.6) (18-20) | 35.43, $p < .001$ | <.001 | .994 | <.001 |
| Trail Making, part A | 153.6 (93.9) (39-300) | 61.4 (40.8) (31-186) | 66.8 (36.0) (30-162) | 12.14, $p < .001$ | <.001 | .961 | <.001 |
| WCST number of categories | 1.9 (1.4) (0-5) | 3.8 (1.4) (1-6) | 3.0 (1.2) (1-5) | 8.74, $p < .001$ | .049 | .119 | <.001 |
| WCST attempts to category | 12.8 (11.3) (6-41) | 11.5 (7.8) (2-37) | 12.6 (6.5) (6-31) | 0.14, n.s | .997 | .900 | .900 |

FAD = FAD patients, AC = asymptomatic carriers, HC = healthy controls

Significant age effect similar across all groups was found in FA values of bilateral Broca's area, right superior longitudinal fasciculus, left inferior longitudinal fasciculus, left inferior fronto-occipital fasciculus, left uncinate fasciculus, bilateral corticospinal tract, left genu, and bilateral frontal white matter (Table 6). In all areas, higher age was related to lower FA value. In addition, a significant interaction effect of FAD patient group and age was found in right cingulate part of cingulum with lower FA values related to higher age in FAD patient group only suggesting that this age effect was due to the progress of the disease and not age.

In $\overline{D}$ values, significant age effect similar across all groups was found in bilateral anterior PFC, bilateral superior longitudinal fasciculus, left inferior longitudinal fasciculus, left uncinate fasciculus, right genu, bilateral frontal white matter, bilateral parietal white matter, left temporal white matter, and bilateral centrum semiovale (Table 7). In all areas, higher age was related to higher $\overline{D}$ value. In addition, a significant interaction

Table 6: Group comparisons of FA values.

| ROI | | FAD | AC | HC | Main effects ($p$) | | | | Interaction effects ($p$) | | Model fit | |
|---|---|---|---|---|---|---|---|---|---|---|---|---|
| | | Mean (sd) | Mean (sd) | Mean (sd) | Age | AC vs HC | FAD vs HC | FAD vs AC | age × AC | age × FAD | $p$ | $R^2$ |
| DL-PFC | left | 0.24 (0.05) | 0.25 (0.04) | 0.26 (0.04) | - | - | - | - | - | - | n.s. | |
| | right | 0.26 (0.04) | 0.27 (0.05) | 0.27 (0.04) | - | - | - | - | - | - | n.s. | |
| A-PFC | left | 0.23 (0.03) | 0.25 (0.04) | 0.25 (0.40) | - | - | - | - | - | - | n.s. | |
| | right | 0.25 (0.05) | 0.27 (0.05) | 0.28 (0.05) | - | - | - | - | - | - | n.s. | |
| BR-PFC | left | 0.32 (0.05) | 0.35 (0.04) | 0.33 (0.05) | .007 | n.s. | n.s. | n.s. | n.s. | n.s. | .010 | 0.142 |
| | right | 0.22 (0.03) | 0.24 (0.03) | 0.22 (0.04) | .005 | n.s. | n.s. | n.s. | n.s. | n.s. | .021 | 0.117 |
| SLF | left | 0.29 (0.03) | 0.30 (0.03) | 0.28 (0.03) | - | - | - | - | - | - | n.s. | |
| | right | 0.34 (0.05) | 0.33 (0.04) | 0.32 (0.05) | <.001 | n.s. | .008 | n.s. | n.s. | n.s. | .004 | 0.171 |
| ILF | left | 0.33 (0.04) | 0.36 (0.06) | 0.36 (0.04) | .016 | n.s. | n.s. | n.s. | n.s. | n.s. | .019 | 0.121 |
| | right | 0.36 (0.04) | 0.38 (0.05) | 0.37 (0.04) | - | - | - | - | - | - | n.s. | |
| IFO | left | 0.24 (0.05) | 0.28 (0.07) | 0.26 (0.04) | .043 | n.s. | n.s. | n.s. | n.s. | n.s. | .015 | 0.129 |
| | right | 0.25 (0.05) | 0.29 (0.07) | 0.27 (0.06) | - | - | - | - | - | - | n.s. | |
| UNC | left | 0.29 (0.07) | 0.31 (0.05) | 0.34 (0.06) | .009 | .014 | n.s. | .024 | n.s. | n.s. | .004 | 0.170 |
| | right | 0.36 (0.05) | 0.36 (0.05) | 0.38 (0.06) | - | - | - | - | - | - | n.s. | |
| CGH | left | 0.28 (0.03) | 0.31 (0.04) | 0.32 (0.05) | n.s. | n.s. | .012 | .020 | n.s. | n.s. | .023 | 0.097 |
| | right | 0.25 (0.03) | 0.28 (0.04) | 0.27 (0.03) | - | - | - | - | - | - | n.s. | |
| CGC | left | 0.36 (0.07) | 0.42 (0.05) | 0.38 (0.06) | n.s. | .042 | <.001 | n.s. | n.s. | n.s. | .010 | 0.125 |
| | right | 0.37 (0.08) | 0.39 (0.05) | 0.36 (0.05) | n.s. | n.s. | .020 | n.s. | .032 | n.s. | .036 | 0.122 |
| FX | | 0.36 (0.12) | 0.35 (0.08) | 0.37 (0.11) | - | - | - | - | - | - | n.s. | |
| ATR | left | 0.36 (0.04) | 0.34 (0.05) | 0.35 (0.04) | - | - | - | - | - | - | n.s. | |
| | right | 0.35 (0.03) | 0.34 (0.05) | 0.34 (0.04) | - | - | - | - | - | - | n.s. | |
| CST | left | 0.28 (0.03) | 0.31 (0.05) | 0.30 (0.04) | .041 | n.s. | n.s. | n.s. | n.s. | n.s. | .009 | 0.148 |
| | right | 0.25 (0.04) | 0.29 (0.03) | 0.28 (0.04) | .026 | n.s. | n.s. | n.s. | n.s. | n.s. | <.001 | 0.294 |
| GCC | left | 0.55 (0.06) | 0.58 (0.04) | 0.59 (0.06) | .025 | n.s. | n.s. | n.s. | n.s. | n.s. | .014 | 0.132 |
| | right | 0.48 (0.05) | 0.50 (0.05) | 0.49 (0.05) | - | - | - | - | - | - | n.s. | |
| SCC | left | 0.47 (0.07) | 0.48 (0.07) | 0.47 (0.07) | - | - | - | - | - | - | n.s. | |
| | right | 0.58 (0.11) | 0.62 (0.09) | 0.59 (0.10) | - | - | - | - | - | - | n.s. | |
| CS | left | 0.26 (0.03) | 0.24 (0.03) | 0.25 (0.02) | - | - | - | - | - | - | n.s. | |
| | right | 0.26 (0.04) | 0.29 (0.04) | 0.28 (0.03) | - | - | - | - | - | - | n.s. | |
| F-WM | left | 0.22 (0.04) | 0.24 (0.03) | 0.24 (0.03) | <.001 | n.s. | n.s. | n.s. | n.s. | n.s. | .001 | 0.216 |
| | right | 0.22 (0.06) | 0.22 (0.03) | 0.23 (0.03) | <.001 | .030 | n.s. | n.s. | n.s. | n.s. | <.001 | 0.223 |
| P-WM | left | 0.31 (0.04) | 0.33 (0.06) | 0.33 (0.03) | - | - | - | - | - | - | n.s. | |
| | right | 0.32 (0.07) | 0.36 (0.08) | 0.34 (0.06) | - | - | - | - | - | - | n.s. | |
| T-WM | left | 0.26 (0.02) | 0.28 (0.04) | 0.28 (0.04) | - | - | - | - | - | - | n.s. | |
| | right | 0.27 (0.04) | 0.29 (0.03) | 0.28 (0.02) | - | - | - | - | - | - | n.s. | |

FAD = FAD patients, AC = asymptomatic carriers, HC = healthy controls

$R^2$ values shown are adjusted

effect of FAD patient group and age was found in bilateral dorsolateral PFC, left Broca's area, left hippocampal part of cingulum, bilateral corticospinal tract, left genu, left frontal white matter, and right temporal white matter with higher $\overline{D}$ values related to higher age in FAD patient group only suggesting that this age effect was due to the progress of the

Table 7: Group comparisons of $\overline{D}$ values.

| ROI | | FAD Mean (sd) $\times 10^{-6}$ | AC Mean (sd) $\times 10^{-6}$ | HC Mean (sd) $\times 10^{-6}$ | Main effects ($p$) Age | AC vs HC | FAD vs HC | FAD vs AC | Interaction effects ($p$) age × AC | age × FAD | Model fit $p$ | $R^2$ |
|---|---|---|---|---|---|---|---|---|---|---|---|---|
| DL-PFC | left | 728 (52) | 700 (28) | 692 (39) | n.s. | n.s. | <.001 | n.s. | n.s. | <.001 | <.001 | 0.370 |
| | right | 725 (45) | 690 (28) | 684 (39) | n.s. | n.s. | .032 | n.s. | n.s. | .010 | <.001 | 0.268 |
| A-PFC | left | 726 (57) | 695 (40) | 698 (36) | .034 | n.s. | .043 | n.s. | n.s. | .039 | <.001 | 0.317 |
| | right | 724 (42) | 703 (34) | 696 (40) | .027 | n.s. | n.s. | n.s. | n.s. | n.s. | .017 | 0.124 |
| BR-PFC | left | 704 (34) | 677 (24) | 675 (28) | n.s. | n.s. | .026 | n.s. | n.s. | .011 | <.001 | 0.295 |
| | right | 675 (32) | 666 (26) | 656 (30) | - | - | - | - | - | - | n.s. | |
| SLF | left | 733 (42) | 710 (32) | 704 (34) | .029 | n.s. | n.s. | n.s. | n.s. | n.s. | .010 | 0.142 |
| | right | 687 (47) | 670 (35) | 670 (34) | .007 | n.s. | n.s. | n.s. | n.s. | n.s. | .021 | 0.117 |
| ILF | left | 808 (48) | 780 (47) | 774 (42) | <.001 | n.s. | n.s. | n.s. | n.s. | n.s. | <.001 | 0.286 |
| | right | 758 (46) | 744 (35) | 749 (38) | - | - | - | - | - | - | n.s. | |
| IFO | left | 834 (37) | 825 (40) | 829 (44) | - | - | - | - | - | - | n.s. | |
| | right | 810 (43) | 787 (28) | 794 (35) | - | - | - | - | - | - | n.s. | |
| UNC | left | 760 (44) | 755 (29) | 745 (35) | .001 | n.s. | n.s. | n.s. | n.s. | n.s. | .006 | 0.159 |
| | right | 735 (39) | 737 (31) | 730 (37) | - | - | - | - | - | - | n.s. | |
| CGH | left | 817 (44) | 785 (32) | 771 (44) | n.s. | n.s. | .021 | n.s. | n.s. | .009 | <.001 | 0.372 |
| | right | 777 (47) | 728 (35) | 733 (29) | n.s. | n.s. | <.001 | <.001 | n.s. | n.s. | <.001 | 0.237 |
| CGC | left | 709 (50) | 674 (30) | 665 (56) | n.s. | n.s. | .005 | .032 | n.s. | n.s. | .015 | 0.110 |
| | right | 681 (62) | 657 (37) | 662 (38) | - | - | - | - | - | - | n.s. | |
| FX | | 989 (130) | 891 (90) | 899 (93) | n.s. | n.s. | .011 | .006 | n.s. | n.s. | .011 | 0.121 |
| ATR | left | 709 (40) | 716 (34) | 708 (35) | - | - | - | - | - | - | n.s. | |
| | right | 697 (32) | 698 (36) | 690 (29) | - | - | - | - | - | - | n.s. | |
| CST | left | 718 (50) | 712 (32) | 708 (18) | n.s. | n.s. | .005 | n.s. | n.s. | .004 | .031 | 0.130 |
| | right | 702 (36) | 678 (24) | 688 (23) | n.s. | n.s. | .002 | n.s. | n.s. | .001 | .002 | 0.237 |
| GCC | left | 766 (85) | 710 (47) | 705 (45) | n.s. | n.s. | .017 | n.s. | n.s. | .009 | <.001 | 0.382 |
| | right | 808 (12) | 733 (63) | 734 (53) | <.001 | n.s. | n.s. | n.s. | n.s. | n.s. | <.001 | 0.304 |
| SCC | left | 733 (57) | 688 (33) | 699 (31) | n.s. | n.s. | .012 | <.001 | n.s. | n.s. | .004 | 0.151 |
| | right | 706 (49) | 688 (38) | 705 (39) | - | - | - | - | - | - | n.s. | |
| CS | left | 751 (35) | 732 (31) | 720 (32) | .038 | n.s. | n.s. | n.s. | n.s. | .018 | .006 | 0.161 |
| | right | 670 (53) | 679 (43) | 685 (31) | .012 | n.s. | n.s. | n.s. | n.s. | n.s. | .035 | 0.099 |
| F-WM | left | 751 (53) | 723 (37) | 719 (39) | .024 | n.s. | .021 | n.s. | n.s. | n.s. | <.001 | 0.364 |
| | right | 778 (46) | 747 (40) | 746 (38) | .004 | n.s. | n.s. | n.s. | n.s. | n.s. | <.002 | 0.202 |
| P-WM | left | 819 (55) | 764 (35) | 771 (43) | .001 | n.s. | n.s. | n.s. | n.s. | n.s. | <.001 | 0.326 |
| | right | 827 (60) | 759 (53) | 772 (51) | .012 | n.s. | n.s. | n.s. | n.s. | .013 | <.001 | 0.275 |
| T-WM | left | 819 (62) | 785 (53) | 778 (51) | .034 | n.s. | .016 | n.s. | n.s. | n.s. | .017 | 0.125 |
| | right | 761 (60) | 739 (33) | 735 (37) | - | - | - | - | - | - | n.s. | |

FAD = FAD patients, AC = asymptomatic carriers, HC = healthy controls

$R^2$ values shown are adjusted

disease and not age. Furthermore, an interaction effect of FAD patient group and age was found in left anterior PFC in addition to the significant age effect across groups. This interaction effect revealed that the effect of age in $\overline{D}$ values was more prominent in FAD patient group than in the other two groups.

Group comparisons between asymptomatic carriers and controls showed that controls had higher FA in left uncinate fasciculus and right frontal white matter, but asymptomatic carriers had higher FA in left cingulate part of cingulum (see Table 6). $\overline{D}$ values did not differ between asymptomatic carriers and controls.

Group comparisons between FAD patients and controls showed that controls had higher FA in left hippocampal cingulum but in fact FAD patients had higher FA in right superior longitudinal fasciculus and also to a small but significant extent in right cingulate part of cingulum (see Table 6). The latter two effects were further examined for the effect of possible outliers, but even though in two control participants had very low FA values in right cingulate part of cingulum, removing these participants did not affect the direction of the effect. [1]

Controls had lower $\overline{D}$ than FAD patients in bilateral dorsolateral PFC, left anterior PFC, left Broca's area, bilateral hippocampal part of cingulum, left cingulate part of cingulum, fornix, bilateral corticospinal tract, left genu, left splenium, left frontal white matter, and right temporal white matter (see Table 7).

Group comparisons between FAD patients and asymptomatic carriers showed that asymptomatic carriers had higher FA in left hippocampal part of cingulum, left cingulate part of cingulum, and right frontal white matter (see Table 6). Asymptomatic carriers had lower $\overline{D}$ than FAD patients in right hippocampal part of cingulum, left cingulate part of cingulum, and fornix (see Table 7).

## 7.3 Relationship between DTI indices and behavioural tasks

The main aim of the analysis was to identify the ROIs which might be related to deficits in binding task performance especially in the asymptomatic carrier group. Thus, based on behavioural results (see Section 7.1) and previous studies (Parra et al. 2010, Parra et al. 2011) the two visual STM binding tasks–shape-colour binding and colour-colour binding–were chosen for further analyses. Asymptomatic carriers show deficits in these tasks despite normal performance in other tasks so it was of interest to examine whether the performance deficits might be related to differences in brain white matter integrity. Also, PAL task was included as a comparison given its wide use in the study of AD and suggested sensitivity to the preclinical phase of the disease.

Base models for the behavioural tasks showed a significant group effect in the shape-colour binding task, colour-colour binding task, and PAL task (see Table 8).

[1] Similar checks were run also to identify other extreme outliers and for their possible causes and effects for the analyses. No systematic error was found to underlie the outliers, thus, they were not excluded from the analysis.

Table 8: Base models for the behavioural tasks.

| | Coefficients | | | $p$ values | | |
|---|---|---|---|---|---|---|
| Task | HC $\beta_0$ | AC $\beta_1$ | FAD $\beta_2$ | AC | FAD | $R^2$ |
| Shape-colour binding | 84.14 | -12.35 | -25.48 | .001 | <.001 | 0.417 |
| Colour-colour binding | 81.48 | -12.25 | -22.31 | .002 | <.001 | 0.357 |
| PAL | 14.19 | -0.47 | -7.02 | ns | <.001 | 0.430 |

FAD = FAD patients, AC = asymptomatic carriers, HC = healthy controls

$R^2$ values shown are adjusted

For the shape-colour binding task, the significant effects of group, ROI, and group × ROI interaction are shown in Table 9. Lower $\overline{D}$ of right anterior PFC was related to higher tasks scores across all groups. In addition, lower FA of left corticospinal tract and higher $\overline{D}$ of right frontal white matter were related to higher task score in control group. However, in these areas an opposite trend was seen in asymptomatic carrier and FAD patient groups where higher FA of left corticospinal tract and lower $\overline{D}$ of right frontal white matter were related to higher task score. Also, in FAD group only higher $\overline{D}$ in left frontal white matter and bilateral genu was related to higher task score, whereas in the other two groups no relationship between these areas and task scores was significant. The regions with significant interaction effects are shown in Figure 5.

Table 9: Linear regression models for shape-colour binding task. Only the statistically significant models are displayed. All models $p < .001$.

| | Main effects ($p$) | | | Interaction effects ($p$) | | |
|---|---|---|---|---|---|---|
| ROI | AC | FAD | ROI | ROI × AC | ROI × FAD | $R^2$ |
| FA left CST | .010 | <.001 | .023 | .030 | .005 | 0.494 |
| $\bar{D}$ right A-PFC | .002 | <.001 | .025 | n.s. | n.s. | 0.464 |
| $\bar{D}$ left F-WM | n.s. | .014 | n.s. | n.s. | .005 | 0.485 |
| $\bar{D}$ right F-WM | .047 | .001 | .024 | .030 | <.001 | .533 |
| $\bar{D}$ left GCC | n.s. | n.s. | n.s. | n.s. | .019 | .488 |
| $\bar{D}$ right GCC | n.s. | n.s. | n.s. | n.s. | .026 | 0.481 |

FAD = FAD patients, AC = asymptomatic carriers, HC = healthy controls

$R^2$ values shown are adjusted

For the colour-colour binding task, the significant effects of group, ROI, and group × ROI interaction are shown in Table 10. There were no effects in FA values of any ROIs. Lower $\overline{D}$ in anterior PFC, bilateral genu and left parietal white matter was related to higher task score across all groups. However, in control group, higher $\overline{D}$ was related to higher task score, whereas the opposite was true in FAD patient group with lower $\overline{D}$ in both of these areas being related to higher task score. In asymptomatic carrier group, similar effects than those in FAD patient group were seen in right frontal white matter but no relationship between $\overline{D}$ value and task score was found in right dorsolateral PFC. Furthermore, while control group showed no significant relationship between $\overline{D}$ values

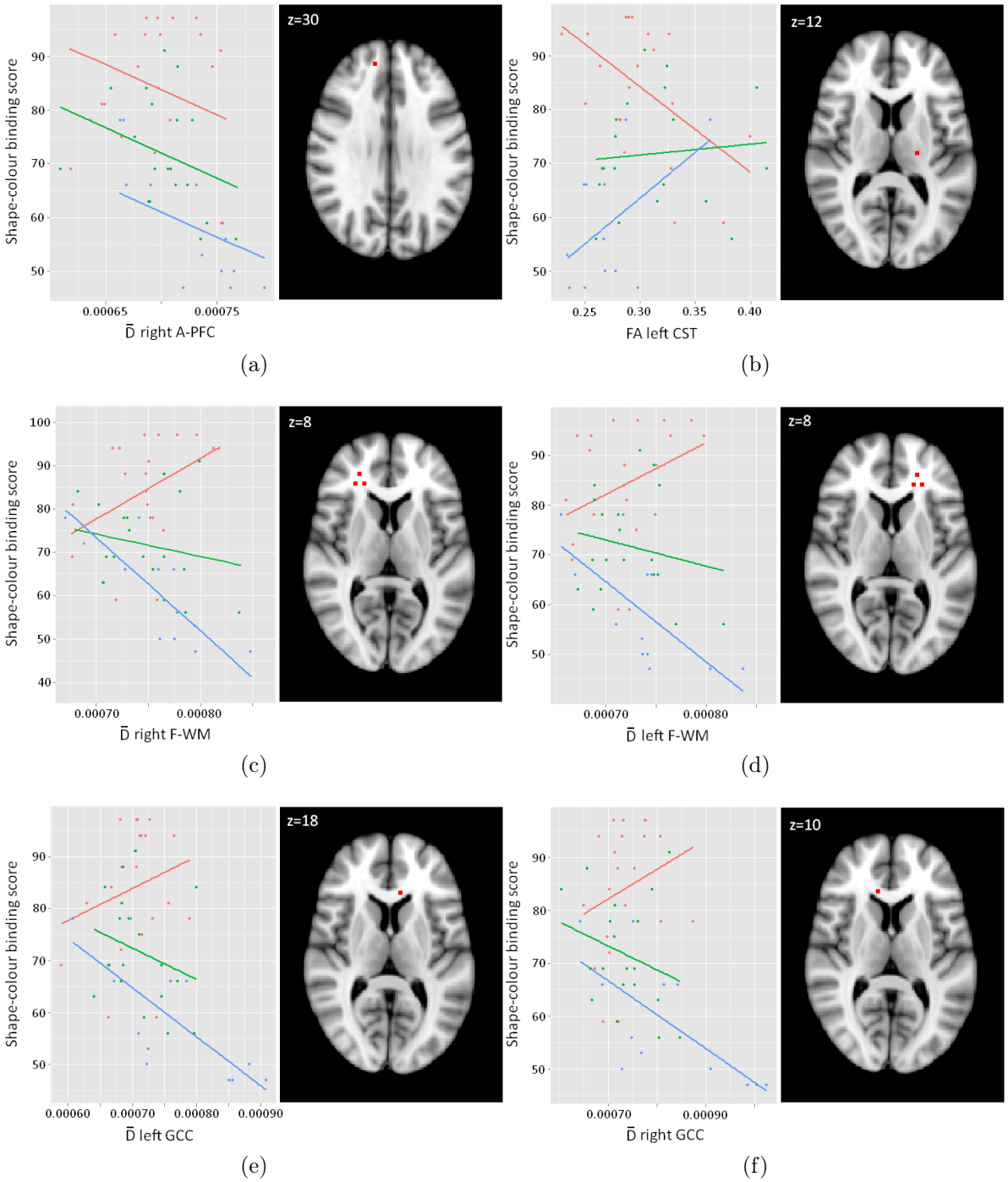


Figure 5: Significant linear regression models for the shape-colour binding task. Left: fitted regression lines; red = controls, green = asymptomatic carriers, blue = FAD patients. Right: the corresponding ROI in standard space. Whenever ROIs were placed on two or more consecutive slices, only one slice is shown as an example. For details, see Table 2 and Appendix B. (a) All groups show a similar significant ROI effect. (b)–(c) All groups show different significant ROI effects. (d)–(f) Only FAD patients show a significant ROI effect.

in right parietal white matter, bilateral splenium or right uncinate fasciculus, in both asymptomatic carrier and FAD patient groups lower $\overline{D}$ was related to higher task score. The regions with significant interaction effects are shown in Figure 6.

Table 10: Linear regression models for colour-colour binding task. Only the statistically significant models are displayed. All models $p < .001$.

| | Main effects ($p$) | | | Interaction effects ($p$) | | |
|---|---|---|---|---|---|---|
| ROI | AC | FAD | ROI | ROI × carrier | ROI × FAD | $R^2$ |
| $\bar{D}$ right A-PFC | .002 | <.001 | .031 | n.s. | n.s. | 40.6 % |
| $\bar{D}$ right DL-PFC | n.s. | .013 | .039 | n.s. | .006 | 42.6 % |
| $\bar{D}$ right F-WM | .019 | .004 | .043 | .012 | .002 | 47.5 % |
| $\bar{D}$ left GCC | .002 | <.001 | .046 | n.s. | n.s. | 39.8 % |
| $\bar{D}$ right GCC | .002 | <.001 | .047 | n.s. | n.s. | 39.7 % |
| $\bar{D}$ left P-WM | <.001 | <.001 | .007 | n.s. | n.s. | 44.0 % |
| $\bar{D}$ right P-WM | .045 | .042 | n.s. | .025 | .018 | 47.2 % |
| $\bar{D}$ left SCC | .013 | .042 | n.s. | .009 | .019 | 45.6 % |
| $\bar{D}$ right SCC | .018 | n.s. | n.s. | .011 | .029 | 45.0 % |
| $\bar{D}$ right UNC | .003 | .040 | n.s. | .002 | .021 | 47.4 % |

FAD = FAD patients, AC = asymptomatic carriers, HC = healthy controls

$R^2$ values shown are adjusted

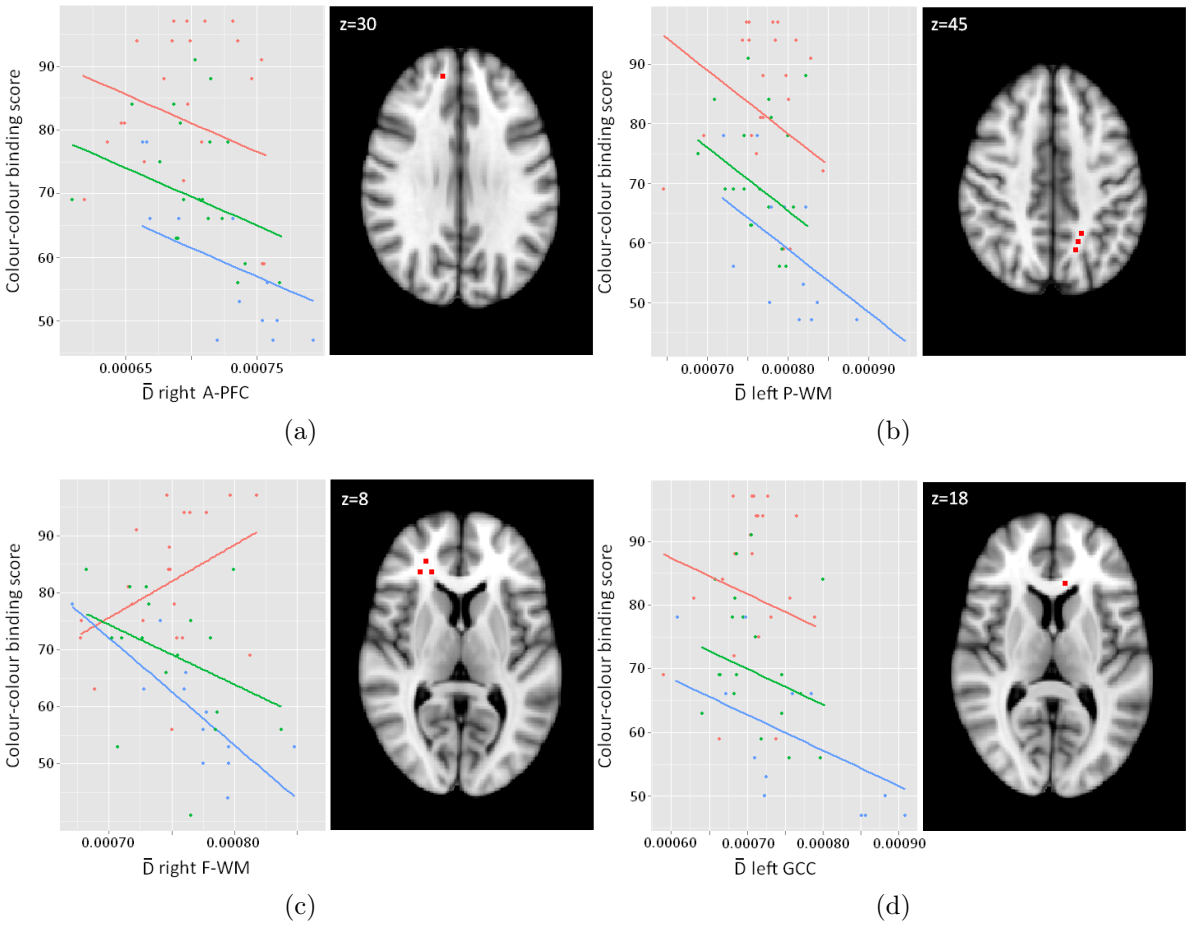


Figure 6: Significant linear regression models for the colour-colour binding task. Left: fitted regression lines; red = controls, green = asymptomatic carriers, blue = FAD patients. Right: the corresponding ROI in standard space. Whenever ROIs were placed on two or more consecutive slices, only one slice is shown as an example. For details, see Table 2 and Appendix B. (a)–(d) All groups show a similar significant ROI effect.

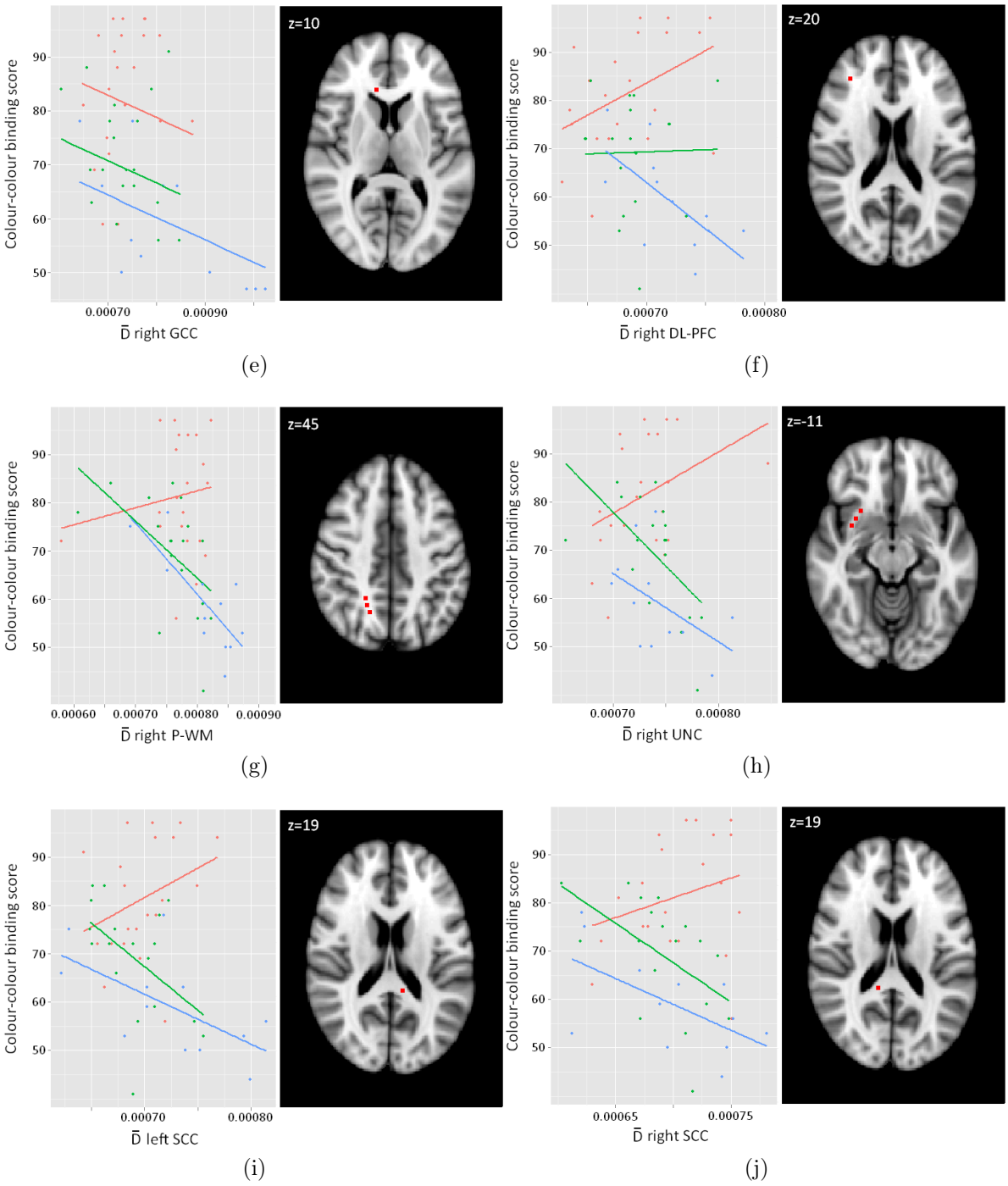


Figure 6: (cont'd) (e) All groups show different significant ROI effects. (f) Only controls and FAD patients show a significant ROI effect. (g)–(j) Only asymptomatic carriers and FAD patients show a significant ROI effect.

For the paired-associates task, the significant effects of group, ROI, and group × ROI interaction are shown in Table 11. Higher FA of right inferior longitudinal fasciculus and bilateral splenium, and lower $\overline{D}$ of right anterior PFC, left Broca's area, left centrum semiovale, left dorsolateral PFC, right frontal white matter, bilateral genu, right inferior longitudinal fasciculus, bilateral parietal white matter, bilateral superior longitudinal fasciculus and right splenium were related to higher task score across all groups. In addition, in control group lower FA of centrum semiovale was related to higher task

score, whereas in asymptomatic carrier and FAD patient group higher FA of this area was related to higher task score. Also, while FA of right frontal white matter and right uncinate fasciculus, and $\overline{D}$ of left hippocampal part of cingulum, left frontal white matter, and left inferior longitudinal fasciculus were not significantly related to task scores in control group, higher FA of right frontal white matter and right uncinate fasciculus and lower $\overline{D}$ of left hippocampal part of cingulum, left frontal white matter and left inferior longitudinal fasciculus were related to higher task scores in asymptomatic carriers group. In FAD patient group, similar effects than those in asymptomatic carrier group were seen in all other areas except for the right uncinate fasciculus where no relationship between FA value and task score were shown (see Figure 7). Different effects across groups are presented in Figure 8.

Table 11: Linear regression models for paired-associates learning task. Only the statistically significant models are displayed. All models $p < .001$.

| | Main effects ($p$) | | | Interaction effects ($p$) | | |
|---|---|---|---|---|---|---|
| ROI | AC | FAD | ROI | ROI × AC | ROI × FAD | $R^2$ |
| FA right CS | .004 | <.001 | .004 | .005 | .002 | 0.536 |
| FA right F-WM | .031 | <.001 | n.s. | .033 | .007 | 0.552 |
| FA right ILF | n.s. | <.001 | .046 | n.s. | n.s. | 0.464 |
| FA left SCC | n.s. | <.001 | .016 | n.s. | n.s. | 0.483 |
| FA right SCC | n.s. | <.001 | .016 | n.s. | n.s. | 0.483 |
| FA right UNC | .016 | n.s. | n.s. | .016 | n.s. | 0.514 |
| $\bar{D}$ right A-PFC | n.s. | <.001 | .008 | n.s. | n.s. | 0.496 |
| $\bar{D}$ left BR-PFC | n.s. | <.001 | .028 | n.s. | n.s. | 0.473 |
| $\bar{D}$ left CGH | n.s. | n.s. | n.s. | .050 | .027 | 0.531 |
| $\bar{D}$ left CS | n.s. | <.001 | .026 | n.s. | n.s. | 0.475 |
| $\bar{D}$ left DL-PFC | n.s. | <.001 | .003 | n.s. | n.s. | 0.516 |
| $\bar{D}$ left F-WM | .027 | n.s. | n.s. | .026 | .024 | 0.526 |
| $\bar{D}$ right F-WM | n.s. | <.001 | .006 | n.s. | n.s. | 0.500 |
| $\bar{D}$ left GCC | n.s. | <.001 | .014 | n.s. | n.s. | 0.486 |
| $\bar{D}$ right GCC | n.s. | <.001 | .035 | n.s. | n.s. | 0.467 |
| $\bar{D}$ left ILF | .028 | n.s. | n.s. | .027 | .027 | 0.516 |
| $\bar{D}$ right ILF | n.s. | <.001 | .038 | n.s. | n.s. | 0.467 |
| $\bar{D}$ left P-WM | n.s. | <.001 | .004 | n.s. | n.s. | 0.509 |
| $\bar{D}$ right P-WM | n.s. | <.001 | <.001 | n.s. | n.s. | 0.534 |
| $\bar{D}$ left SLF | n.s. | <.001 | .034 | n.s. | n.s. | 0.469 |
| $\bar{D}$ right SLF | n.s. | <.001 | .033 | n.s. | n.s. | 0.470 |
| $\bar{D}$ right SCC | n.s. | <.001 | .008 | n.s. | n.s. | 0.495 |

FAD = FAD patients, AC = asymptomatic carriers, HC = healthy controls

$R^2$ values shown are adjusted

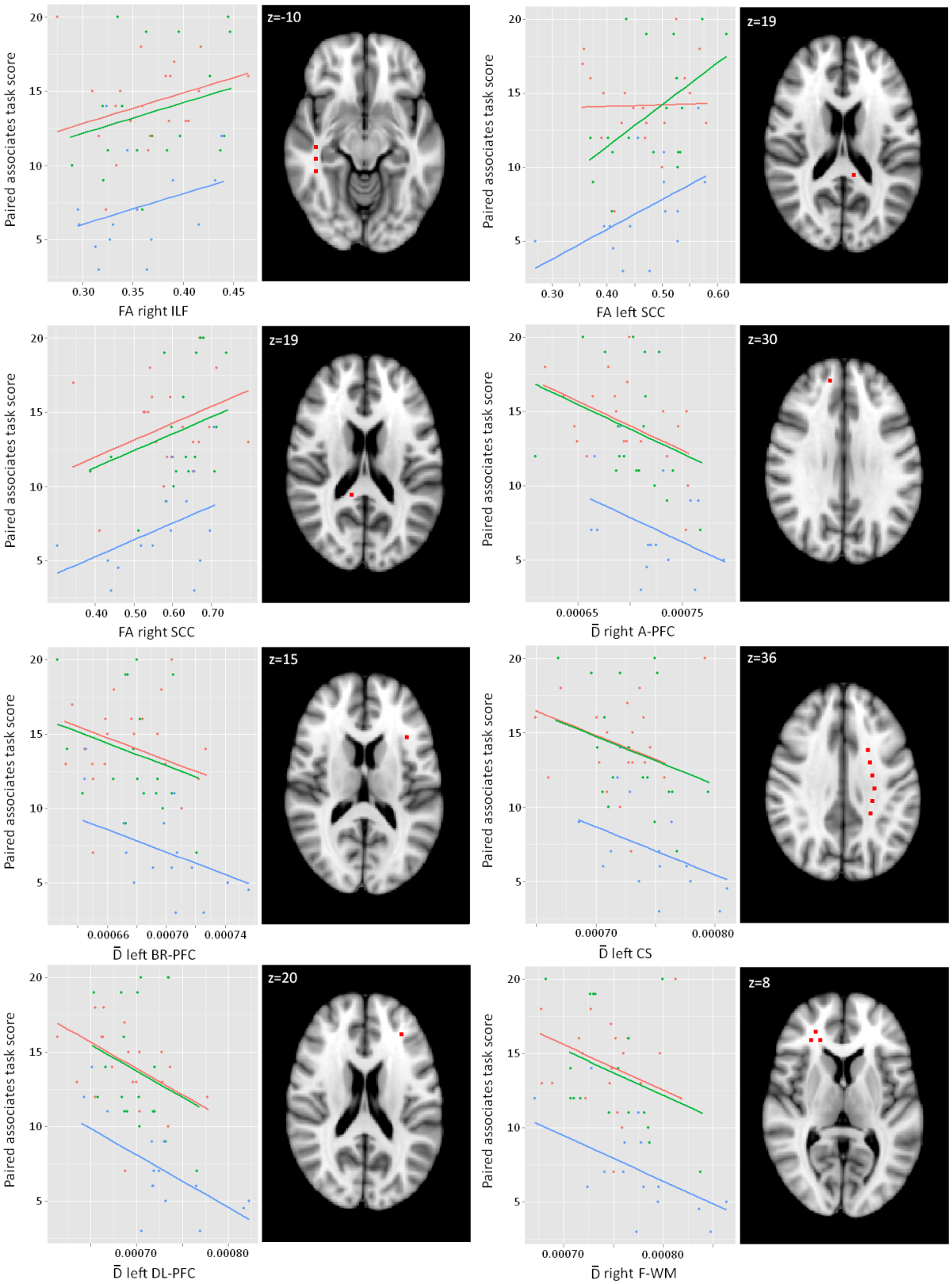


Figure 7: Significant linear regression models with similar effects across groups for the paired-associates task. Left: fitted regression lines; red = controls, green = asymptomatic carriers, blue = FAD patients. Right: the corresponding ROI in standard space. Whenever ROIs were placed on two or more consecutive slices, only one slice is shown as an example. For details, see Table 2 and Appendix B.

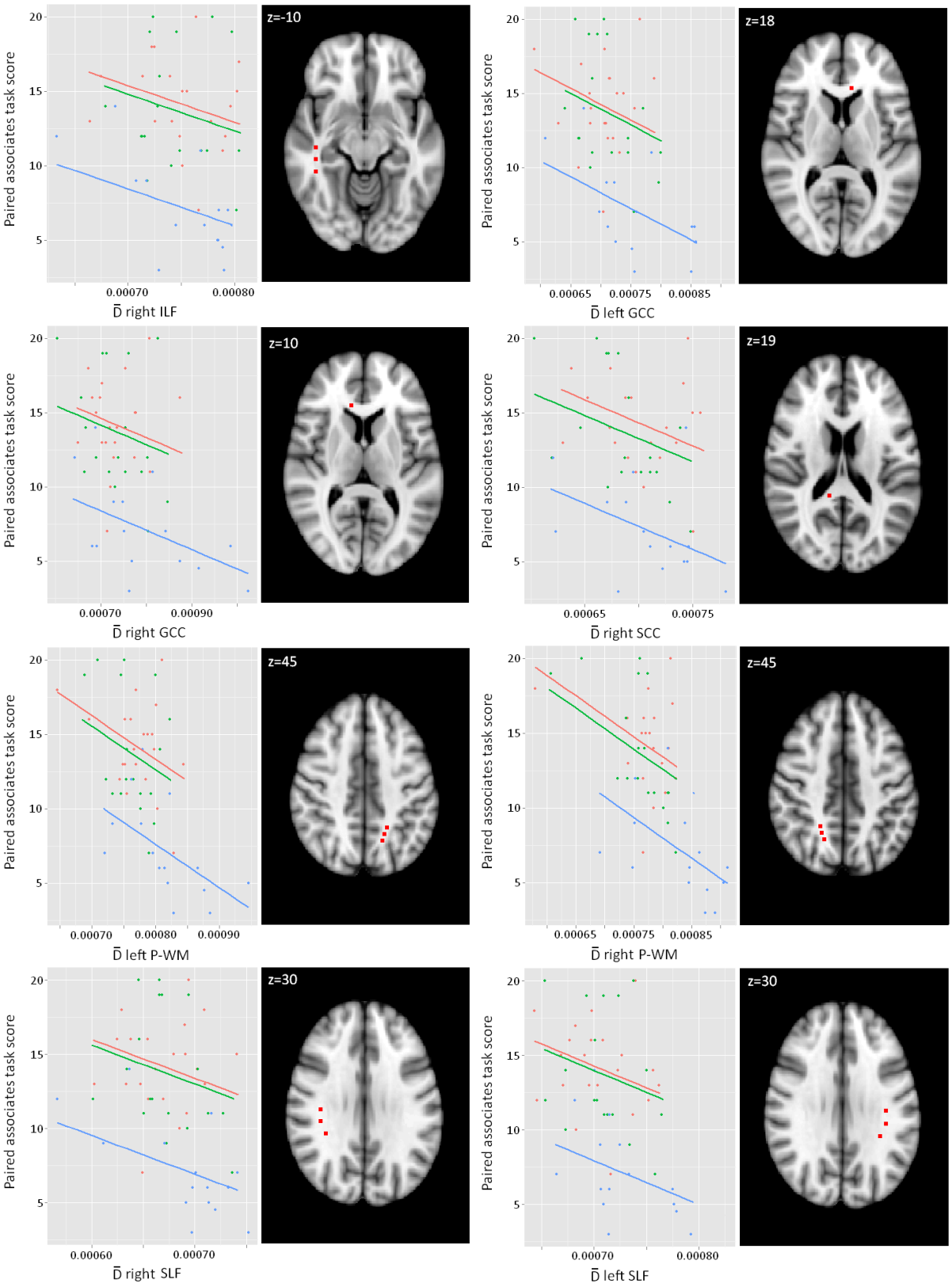


Figure 7: cont'd

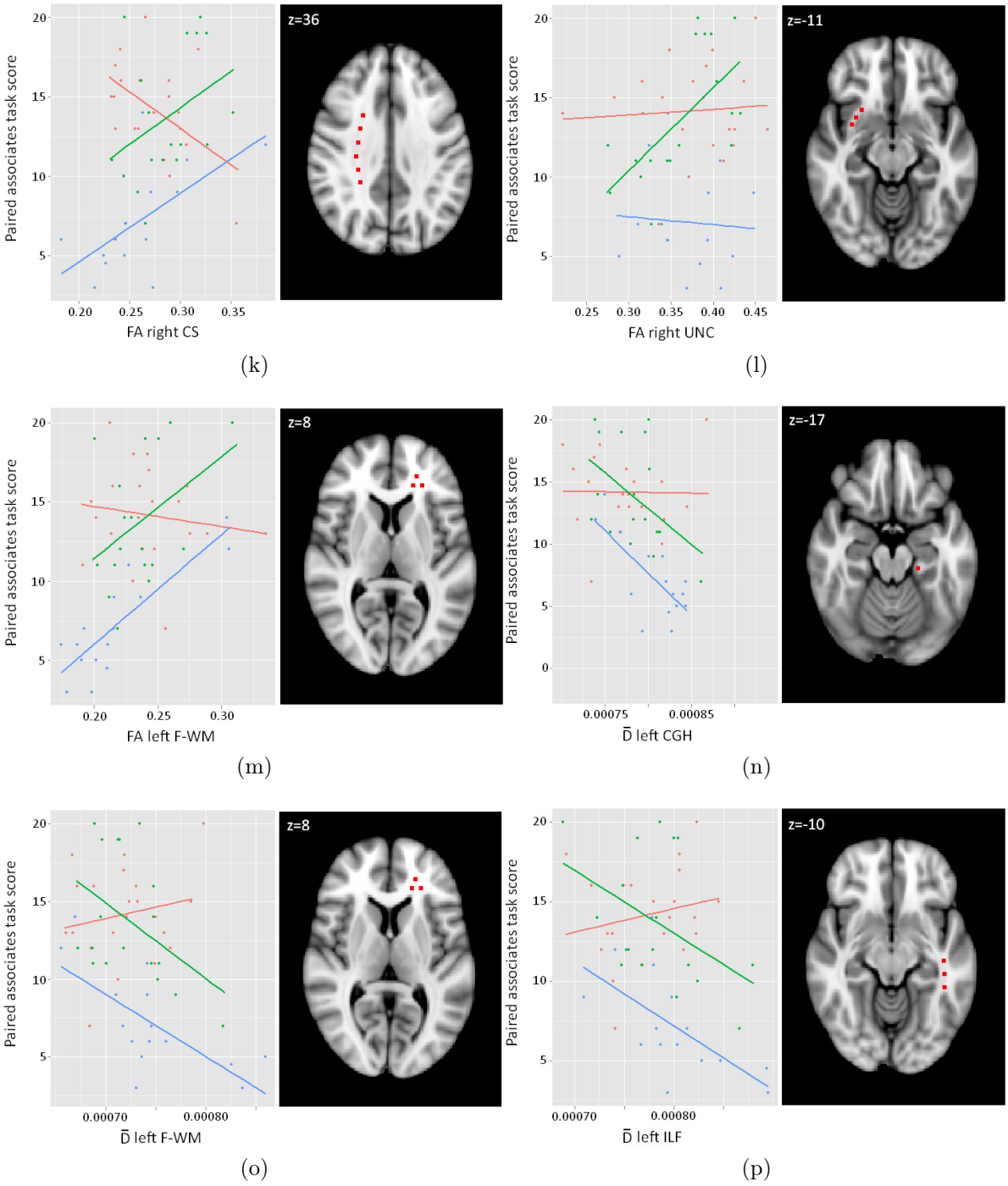


Figure 8: Significant linear regression models with different effects across groups for the paired-associates task. Left: fitted regression lines; red = controls, green = asymptomatic carriers, blue = FAD patients. Right: the corresponding ROI in standard space. Whenever ROIs were placed on two or more consecutive slices, only one slice is shown as an example. For details, see Table 2 and Appendix B. (k) All groups show different significant ROI effects. (l) Only asymptomatic carriers show a significant ROI effect. (m)–(p) Asymptomatic carriers and FAD patients show a significant ROI effect.

# 8 Discussion

This study showed significant differences in white matter integrity related to FAD, some of which are present already in the asymptomatic phase of the disease. Furthermore, behavioural deficits in visual STM tasks in carriers of the gene mutation leading to FAD were accompanied by changes in white matter integrity in several areas.

## 8.1 Group comparisons

Asymptomatic phase of familial AD caused by E280A mutation in presenilin-1 gene is characterized by intact performance in traditional neuropsychological tasks including tests for memory, language, and executive functions; yet, carriers of the gene mutation show impairments in tasks requiring visual STM binding (Parra, Abrahams, Logie, Mendez, et al., 2010; Parra et al., 2011). Our results are consistent with these findings in that the asymptomatic mutation carriers showed no deficits in a neuropsychological test pattern, but were impaired in shape-colour and colour-colour binding conditions.

Changes in white matter integrity in the presymptomatic phase of familial AD have been reported previously only by Ringman et al. (2007). We expanded the investigation of these changes to both FA and $\overline{D}$ values as indexes of white matter integrity and report findings in both asymptomatic and clinical phases of familial AD.

The current results show decreased FA in left uncinate fasciculus and right frontal white matter of left uncinate fasciculus and right frontal white matter of asymptomatic carriers. This seems inconsistent with Ringman et al.'s findings of reduced FA in the fornix and left frontal white matter regions. However, the differences between our and Ringman et al.'s results might be attributed to differences in the choice and placement of regions of interest. Ringman et al. did not include uncinate fasciculus and both frontal white matter and fornix were defined differently to the current study. Furthermore, Ringman et al.'s frontal white matter consisted of two voxels in inferior frontal white matter corresponding best to our anterior PFC area so it is unlikely that we have chosen the exact same voxels that Ringman et al. used. Also, Ringman et al. defined fornix as the two brightest voxels in certain areas of fornix based on the individual FA images whereas we used four voxels placed in T2-weighted images. The latter way is preferred because it minimizes the effect of biasing the FA values by choosing them in the FA map itself (Bozzali & Cherubini, 2007). Taken together, the results from these studies serve as complimentary to each other.

Our finding of reduced FA in right frontal matter in asymptomatic FAD is supported by similar changes in MCI that precedes SAD (Zhuang et al., 2010; Medina et al., 2006). However, there is no evidence for early changes in FA of uncinate fasciculus in MCI studies (Kiuchi et al., 2009; Pievani et al., 2010; Damoiseaux et al., 2009) which suggests that early changes in this region might be specific to early FAD but not to early SAD.

Also, this is to our knowledge the first study to examine changes in white matter integrity in clinical FAD. Namely, decreases in FA were seen in medial temporal lobe structures including left hippocampal and right cingulate parts of cingulum which is in line with the progression of FAD from medial temporal lobes via cingulum and fornix to higher order association areas (Braak et al. 1999; Acosta-Cabronero, Williams, Pengas, & Nestor, 2010).

$\overline{D}$ did not show changes in asymptomatic FAD but asymptomatic carriers and FAD patients did not significantly differ in $\overline{D}$ of left frontal lobe structures, corticospinal tract, and right temporal lobe regions, all of which showed increased $\overline{D}$ in clinical FAD. Therefore, these areas might be slightly affected already in asymptomatic FAD. In addition to these areas, increased $\overline{D}$ in clinical FAD was seen in medial temporal lobe regions including bilateral hippocampal cingulum, left cingulate part of cingulum and fornix, in bilateral frontal areas, and in left splenium. The importance of these regions was also supported by our finding that only FAD patients showed age effects in overlapping areas. Since these seemingly age-related changes were present only in FAD patient group, it is probable that these effects result from the progress of the disease and not from age. However, the effects related to age and disease progress are impossible to separate from each other.

The findings in $\overline{D}$ of medial temporal lobes again support the role of these areas in FAD and AD in general. However, we found wide-spread effects also in frontal regions even though changes in prefrontal cortex have been usually related to age and not to AD specifically (e.g., Head et al., 2004). Despite efforts to control for the age-related effects, it is possible that our results partially reflect the higher age in the FAD patients compared to the other groups thus explaining the extensive differences in frontal areas. Another possibility is that effects in prefrontal areas are specific to FAD and not to SAD. Furthermore, the finding that corticospinal tract was effected in clinical FAD was unexpected given that corticospinal tract and motor functions have shown relative preservation until later phases of AD (e.g., Mielke et al., 2009). However, some studies have demonstrated changes in corticospinal tract in AD and already in MCI (Xie et al., 2006; Zhuang et al., 2010). More research is needed to identify the areas affected in the course of FAD and how these correspond to the changes in SAD.

Against our hypotheses, increased FA in right superior longitudinal fasciculus and right cingulate part of cingulum were seen in clinical FAD. Our finding in right cingulate part of cingulum is especially difficult to explain given the presence of increased $\overline{D}$ in the same area; however, there was large individual variation in FAD patient group in the values of this area which might explain the results. On the other hand, increased FA was found also in right superior longitudinal fasciculus, a tract that connects frontal, parietal, temporal and occipital lobes. An unexpected increase in FA has also been recently by Douaud et al. (2011) who showed increased FA in the centrum semiovale of MCI patients. Increase in FA is controversial given that neuropathological processes should lead to decrease in

FA (Concha, Gross, Wheatley, & Beaulieu, 2006). Increased FA in clinical FAD can thus be explained in at least two different ways. First, the pathological processes in FAD might show a distinct pattern and actually increase white matter integrity in some areas. Second, given the plasticity of the nervous system increased FA in clinical FAD might reflect the need for compensatory networds taking over while other areas show neural damage. Compatible with better white matter integrity in superior longitudinal fasciculus, frontoparietal network increases its activation in compensation of reduced functionality of medial temporal lobe structures (e.g., Pariente et al., 2005). This possibility leaves out several questions related to the plasticity of white matter structures but has potential for further research.

## 8.2 Behavioural tasks and DTI indices

This is to our knowledge the first study to combine white matter integrity indices to task performance in visual STM binding task. Furthermore, we report the first results concerning the possible neuroanatomical background underlying STM binding problems in FAD. Group differences explained most of the variance in both visual STM binding tasks and paired-associates task which was used for comparison. In addition, white matter integrity of different areas added to the explained variance differently in binding tasks and paired-associates task, and also differently in controls and asymptomatic and clinical FAD.

We observed three different patterns of relationships between white matter integrity and task performance. First, some areas had a similar relationship to task performance across all groups. Second, some area did not show a relationship with task performance in healthy controls but were involved in the task performance in asymptomatic and clinical FAD. Third, the relationships of certain areas and task performance were opposite between healthy controls and asymptomatic and clinical FAD groups. These effects and their possible implications will be discussed next.

First, in both visual STM binding tasks and paired-associates task there were some areas that were equally important for task performance in all groups. Similar relationship across groups suggests that white matter integrity in these areas is important for normal task performance and not to FAD impairments.

Better performance across all groups in both visual STM tasks was related to better white matter integrity in right anterior PFC. Functional neuroimaging studies have shown activation of anterior PFC in most cognitive tasks suggesting that it might reflect monitoring of both external and internal input (Burgess, Dumontheil, & Gilbert, 2007). Thus, it is possible that the relationship between white matter integrity of anterior PFC and task performance in this study reflects the general monitoring and attentional demands of the binding task which are known to be important for binding (Zimmer et al., 2006). Colour-colour binding task performance was also related to white matter integrity in another frontal area, genu of corpus callosum that connects the two hemispheres in the area of

frontal lobes. The importance of the prefrontal white matter integrity to STM binding performance is consistent with the results from fMRI studies showing prefrontal cortex activation during visual STM binding tasks (Sala & Courtney, 2007; Prabhakaran et al., 2000; Achim & Lepage, 2005; Piekema et al., 2010).

In addition to the prefrontal white matter regions, colour-colour binding performance was also related to the white matter integrity of left parietal white matter. Previous studies have shown the importance of parietal cortex in extrinsic intra-item binding including colour and location (Uncapher et al., 2006; Piekema et al., 2010). Thus, we report the importance of parietal areas also in extrinsic intra-item binding including two colours.

Performance in paired-associates task was related to frontal white matter areas including left dorsolateral PFC, right frontal white matter, and bilateral genu, to parietal areas including bilateral parietal white matter and right splenium, to white matter tracts including bilateral superior longitudinal fasciculus and right inferior longitudinal fasciculus, and to left centrum semiovale. The involvement of left frontal areas, parietal areas and superior and inferior longitudinal fasciculus can result from the importance of phonological storage and rehearsal during the verbal PAL task since the phonological storage in parietal areas or superior temporal lobe (Paulesu, Frith, & Frackowiak, 1993; E. Smith & Jonides, 1997; Buchsbaum & D'Esposito, 2008), and rehearsal in a network consisting of Broca's area, premotor cortex, supplementary motor areas and cerebellum (Paulesu et al., 1993, Smith & Jonides, 1997).

The second and third patterns, where healthy controls show either no effect or a negative effect of white matter integrity for task performance, respectively, when a positive relationship in FAD groups is present, are closely related. When controls show no relationship between white matter integrity and task performance in areas where there is a relationship between higher white matter integrity and higher task performance in mutation carrier groups, it is possible that performance in the task in normal population is independent of these areas, but that mutation carrier groups can benefit from the additional involvement of these areas in the task. Mutation carriers might try to use these additional areas to compensate for the difficulties in task performance. The finding that in same regions control group shows a relationship between *lower* white matter integrity in certain areas and higher task performance is more puzzling. This might be just a stronger case of independence of the white matter integrity in these areas in control group. Another possibility is that weak connections in these areas do help with task performance in the form of less interfering 'noise' from task-irrelevant regions. However, in mutation carrier groups where performance is already impaired these additional resources might be need for the best task performance.

In both patterns of differences, there are at least two possible interpretations for the group differences. First, it is possible that groups use altogether different strategies to complete the task. Second, it is also possible that the differences stem from functional compensation for neuropathological changes associated with AD.

The areas showing no relationship between controls and white matter integrity but a positive relationship in FAD between higher white matter integrity and better task performance did not overlap between the two visual STM binding tasks. In shape-colour binding, these effects were seen in frontal areas including left frontal white matter and bilateral genu, and in colour-coloug binding task in parietal areas including right parietal white matter and left splenium of corpus callosum, and in right uncinate fasciculus that connects ventromedial PFC to medial temporal lobes. Thus, in shape-colour binding task the importance of additional frontal areas was emphasised, whereas in colour-colour binding task parietal regions were more important, consistently with the findings of importance of frontal areas in shape-colour binding and frontal and parietal areas in colour-colour binding presented above.

Also, in both visual STM binding tasks the right frontal white matter showed an opposite relationship to task performance between healthy controls and mutation carrier groups. The importance of right frontal white matter for the performance of visual STM binding is again emphasized with mutation carriers showing potentially more frontal involvement in binding tasks. One possible explanation for the frontal involvement is that because of difficulties in the task, mutation carriers need additional cognitive resources to complete the task. Right frontal areas have been linked to the visuospatial short term storage (Jonides et al., 1993) and it is possible that mutation carriers rely more on this resource whereas the task is easier for healthy controls with no need for additional resources.

In shape-colour binding task, an opposite relationship to task performance in controls and FAD patients was also present in left corticospinal tract. This finding of the possible importance of left corticospinal tract for the shape-colour task performance in FAD patient group is somewhat unexpected. Motor functions are considered to be largely preserved in AD (e.g., Mielke et al., 2009) and so far there is no evidence for the importance of motor regions in the performance of shape-colour binding task. Given that this particular task has not yet been used in functional neuroimaging studies, it is not yet clear what the meaning of this result is.

Taken together, performance in shape-colour binding task seems to be related especially to the white matter integrity of frontal white matter regions, whereas colour-colour binding performance relies on both frontal and parietal white matter regions which supports the previous findings especially of the importance of prefrontal cortex in STM binding (e.g., Prabhakaran et al., 2000). The differences between these two STM binding tasks suggest that the two tasks rely partly on different brain regions. This supports the distinction between intrinsic (here, shape-colour binding) and extrinsic (here, colour-colour binding) intra-item associations and their different neural underpinnings with more parietal involvement in extrinsic intra-item binding (e.g., Uncapher et al., 2006). Also, no relationship was found between the STM binding tasks and medial temporal lobes which supports the previous findings that binding performance is independent of medial temporal lobe structures (Piekema et al., 2006).

In paired-associates task, better performance in both asymptomatic and clinical FAD was related to higher white matter integrity in additional areas including left frontal white matter, left hippocampal cingulum, and left inferior longitudinal fasciculus. Asymptomatic carriers also benefited from higher white matter integrity in uncinate fasciculus. Additionally, the only area with an opposite relationship to task performance in controls and mutation carriers was right centrum semiovale. In general, in paired-associates task the mutation carrier groups showed less involvement of additional areas compared to the large amount of areas that were related to the task performance similarly across all groups.

Thus, similarly to binding tasks, white matter integrity in frontal and parietal white matter regions was also related to performance in the paired-associates task. Additionally, white matter integrity of superior and inferior longitudinal fasciculi were related to task performance, potentially reflecting the use of phonological memory systems in the verbal paired-associates task used here. In addition, in FAD patients also the white matter integrity of medial temporal lobe tracts was related to task performance. This finding supports the previous results on the importance of medial temporal lobes in associative learning (Lowndes & Savage, 2007; Mayes et al., 2007).

The most prominent difference between the visual STM tasks and paired-associates task and their relationship to white matter integrity was in the amount of areas related to task performance across the groups. In paired-associates task a large amount of areas showed similar effects to task performance across all groups, whereas in binding tasks similar effects across groups were seen in only few areas. Thus, performance in paired-associates task relies on more areas than that in binding task. This is at least partially explained by the phonological memory processes required in the paired-associates task in comparison to the purely visual STM binding tasks.

## 8.3 Age effects

Age-related changes have been repeatedly demonstrated especially in anterior brain areas including the frontal lobe white matter and genu of corpus callosum (Head et al., 2004; Davis et al., 2009; Burzynska et al., 2010; Bennett, Madden, Vaidya, Howard, & Howard Jr, 2010; however, see Barrick, Charlton, Clark, & Markus, 2010) and in the tracts leading to and from the frontal lobes such as superior longitudinal fasciculus (Madden et al., 2009; Bennett et al., 2010), sagittal stratum that includes parts of inferior longitudinal fasciculus and fronto-occipital fasciculus (Burzynska et al., 2010; Bennett et al., 2010; Davis et al., 2009), and uncinate fasciculus (Hasan et al., 2009; Davis et al., 2009). Consistent with the previous finding, we found age effects that were similar across all groups in either one or both DTI indices in frontal areas including bilateral Broca's area, anterior PFC, general frontal white matter, genu of corpus callosum, and in white matter tracts leading to and from frontal areas including superior longitudinal fasciculus, left inferior longitudinal fasciculus, left inferior fronto-occipital fasciculus, and left uncinate

fasciculus. In all areas, higher age was associated with reduced white matter integrity as indicated by higher FA values and lower $\overline{D}$ values.

In addition, we found age effects across all groups in the FA of corticospinal tract and $\overline{D}$ of bilateral parietal white matter, centrum semiovale and left temporal white matter. However, the age effects in corticospinal tract and temporal white matter were subtle and, due to the amount of multiple comparisons, should be approached cautiously. On the other hand, the findings in parietal white matter and centrum semiovale are supported by previous research. Even though posterior areas including parietal white matter have shown no effects when the whole lobar white matter was studied (e.g., O'Sullivan et al., 2001), studies using smaller subregions such as pericallosal white matter have reported age-related changes (Bennett et al., 2010). Also, there is evidence for age-related changes in centrum semiovale (Sullivan et al., 2001). Taken together, the age-related changes shown in this study are consistent with previous research. Interestingly, the population used in this study is rather young (mean age of controls 39 years, of asymptomatic carriers 35 years) which suggests that age-related changes can be detected already in the 4th decade of life.

## 8.4 Limitations and future directions

The current study is among the first investigations of white matter changes related to asymptomatic and clinical FAD, and presents first suggestions of the neural underpinnings of the visual STM impairments witnessed in FAD.

However, the current study has also its limitations. First, the quality of the DTI data available in this study was limited and, therefore, the methods used for DTI quantification had to be compromised. Ideally, an explorative study such as this would have benefited from the use TBSS or other voxelwise statistical methods (e.g., Smith et al. 2006). With the lower quality of the data, ROI approach was the only possible way for the DTI data analysis. Since ROI approach is limited by being restricted to only the pre-selected regions, the selection of ROIs was especially important and was carefully planned in this study. In conclusion, while it is possible that not all relevant regions were identified, the large amount of ROIs guaranteed that most of the possibly relevant regions were included. Also, only T2-weighted structural images were available for the dataset instead of the T1-weighted images which possibly would have resulted in better registration between standard space and individual structural images (Smith et al., 2006). Future studies should emphasize the careful collection of DTI data to ensure a high quality and the possibility to use whole-brain methods for the analysis.

In addition, even though the current study extended the investigation of DTI indices in FAD to mean diffusivity, future studies could also investigate the more specific diffusivity measures including radial and axial diffusivity which are simply averaged in the mean diffusivity values. It has been shown that these indices are differently sensitive to changes

in normal ageing (Davis et al., 2009); thus, their role also in SAD and FAD deserves more attention.

Moreover, this study is correlative in that it combines measures of brain anatomy with behavioural performance. Therefore, only tentative interpretations regarding the importance of different brain regions to the task performance can be drawn. In future, the relationship between visual STM binding task performance and white matter integrity in FAD and SAD could be studied using connectivity fMRI simultaneously with the task to observe the importance of the specific regions *in vivo*. The neuroanatomical underpinnings of shape-colour and colour-colour binding tasks have not yet been fully studied in healthy population either, so studies in normal population could potentially shed more light on the reasons why the performance in this task can distinguish FAD already in the asymptomatic phase. A thorough investigation could possibly lead to new ways for the early diagnosis of AD in the future.

Finally, while the current study provides a preliminary exploration of white matter changes in FAD and their possible relationship to visual STM binding deficits, future studies will hopefully add to the current results in forming a clearer picture of the underpinning of FAD. Future studies should aim to recruit larger samples and to plan the use of longitudinal settings to provide a more thorough investigation of the different stages of the disease.

## 8.5 Conclusions

The current study showed that changes in white matter integrity in specific brain regions–including left uncinate fasciculus and right frontal white matter–can precede the FAD diagnosis and will extend to wide-spread areas in the clinical phase of FAD. Also, the behavioural impairments in visual STM tasks that are present already in the asymptomatic phase of FAD might be related to changes in white matter integrity in areas that are important for the performance of these tasks, including especially frontal and parietal regions.

# References

Achim, A., & Lepage, M. (2005). Neural correlates of memory for items and for associations: an event-related functional magnetic resonance imaging study. *Journal of Cognitive Neuroscience*, *17*(4), 652–667.

Acosta-Cabronero, J., Williams, G., Pengas, G., & Nestor, P. (2010). Absolute diffusivities define the landscape of white matter degeneration in alzheimer's disease. *Brain*, *133*(2), 529–539.

Ardila, A., Lopera, F., Rosselli, M., Moreno, S., Madrigal, L., Arango-Lasprilla, J., et al. (2000). Neuropsychological profile of a large kindred with familial Alzheimer's disease caused by the E280A single presenilin-1 mutation. *Archives of Clinical Neuropsychology*, *15*(6), 515–528.

Ashburner, J., & Friston, K. (2000). Voxel-based morphometry–the methods. *NeuroImage*, *11*(6), 805–821.

Avramopoulos, D. (2009). Genetics of Alzheimer's disease: recent advances. *Genome*, *1–7*, 34.

Baddeley, A., Allen, R., & Vargha-Khadem, F. (2010). Is the hippocampus necessary for visual and verbal binding in working memory? *Neuropsychologia*, *48*(4), 1089–1095.

Baron, J., Chetelat, G., Desgranges, B., Perchey, G., Landeau, B., De La Sayette, V., et al. (2001). In vivo mapping of gray matter loss with voxel-based morphometry in mild Alzheimer's disease. *NeuroImage*, *14*(2), 298–309.

Barrick, T., Charlton, R., Clark, C., & Markus, H. (2010). White matter structural decline in normal ageing: A prospective longitudinal study using tract-based spatial statistics. *Neuroimage*, *51*(2), 565–577.

Bartzokis, G., Cummings, J., Sultzer, D., Henderson, V., Nuechterlein, K., & Mintz, J. (2003). White matter structural integrity in healthy aging adults and patients with Alzheimer disease: a magnetic resonance imaging study. *Archives of Neurology*, *60*(3), 393–398.

Basser, P. (1995). Inferring microstructural features and the physiological state of tissues from diffusion-weighted images. *NMR in Biomedicine*, *8*(7), 333–344.

Basser, P. (1997). New histological and physiological stains derived from diffusion-tensor MR images. *Annals of the New York Academy of Sciences*, *820*, 123–138.

Basser, P., & Jones, D. (2002). Diffusion-tensor MRI: theory, experimental design and data analysis–a technical review. *NMR in Biomedicine*, *15*(7-8), 456–467.

Basser, P., Mattiello, J., & LeBihan, D. (1994). MR diffusion tensor spectroscopy and imaging. *Biophysical Journal*, *66*(1), 259–267.

Beaulieu, C. (2002). The basis of anisotropic water diffusion in the nervous system–a technical review. *NMR in Biomedicine*, *15*(7-8), 435–455.

Behrens, T., Johansen-Berg, H., Woolrich, M., Smith, S., Wheeler-Kingshott, C., Boulby,

P., et al. (2003). Non-invasive mapping of connections between human thalamus and cortex using diffusion imaging. *Nature Neuroscience*, *6*(7), 750–757.

Bennett, I., Madden, D., Vaidya, C., Howard, D., & Howard Jr, J. (2010). Age-related differences in multiple measures of white matter integrity: A diffusion tensor imaging study of healthy aging. *Human Brain Mapping*, *31*(3), 378–390.

Berg, E. (1948). A simple objective test for measuring flexibility in thinking. *Journal of General Psychology*, *39*, 15–22.

Bertram, L., & Tanzi, R. (2008). Thirty years of Alzheimer's disease genetics: the implications of systematic meta-analyses. *Nature Reviews Neuroscience*, *9*(10), 768–778.

Bookstein, F. (2001). "Voxel-based morphometry" should not be used with imperfectly registered images. *NeuroImage*, *14*(6), 1454–1462.

Bozzali, M., & Cherubini, A. (2007). Diffusion tensor MRI to investigate dementias: a brief review. *Magnetic Resonance Imaging*, *25*(6), 969–977.

Bozzali, M., Falini, A., Franceschi, M., Cercignani, M., Zuffi, M., Scotti, G., et al. (2002). White matter damage in Alzheimer's disease assessed in vivo using diffusion tensor magnetic resonance imaging. *Journal of Neurology, Neurosurgery & Psychiatry*, *72*(6), 742–746.

Braak, E., Griffing, K., Arai, K., Bohl, J., Bratzke, H., & Braak, H. (1999). Neuropathology of Alzheimer's disease: what is new since A. Alzheimer? *European Archives of Psychiatry and Clinical Neuroscience*, *249*(3), 14–22.

Braak, H., & Braak, E. (1991). Neuropathological stageing of Alzheimer-related changes. *Acta Neuropathologica*, *82*(4), 239–259.

Brockmole, J., Parra, M., Sala, S., & Logie, R. (2008). Do binding deficits account for age-related decline in visual working memory? *Psychonomic Bulletin & Review*, *15*(3), 543–547.

Bronge, L., Bogdanovic, N., & Wahlund, L. (2002). Postmortem MRI and histopathology of white matter changes in Alzheimer brains. *Dementia and Geriatric Cognitive Disorders*, *13*(4), 205–212.

Brookmeyer, R., Johnson, E., Ziegler-Graham, K., & Arrighi, H. (2007). Forecasting the global burden of Alzheimer's disease. *Alzheimer's and Dementia*, *3*(3), 186–191.

Brun, A., & Englund, E. (1986). A white matter disorder in dementia of the Alzheimer type: a pathoanatomical study. *Annals of Neurology*, *19*(3), 253–262.

Buchsbaum, B., & D'Esposito, M. (2008). The search for the phonological store: from loop to convolution. *Journal of Cognitive Neuroscience*, *20*(5), 762–778.

Burgess, P., Dumontheil, I., & Gilbert, S. (2007). The gateway hypothesis of rostral prefrontal cortex (area 10) function. *Trends in Cognitive Sciences*, *11*(7), 290–298.

Burgmans, S., Gronenschild, E., Fandakova, Y., Shing, Y., van Boxtel, M., Vuurman, E., et al. (2011). Age differences in speed of processing are partially mediated by differences in axonal integrity. *NeuroImage*, *55*, 1287–1297.

Burzynska, A., Preuschhof, C., Bäckman, L., Nyberg, L., Li, S., Lindenberger, U., et al. (2010). Age-related differences in white matter microstructure: Region-specific patterns of diffusivity. *NeuroImage*, *49*(3), 2104–2112.

Busatto, G., Garrido, G., Almeida, O., Castro, C., Camargo, C., Cid, C., et al. (2003). A voxel-based morphometry study of temporal lobe gray matter reductions in Alzheimer's disease. *Neurobiology of Aging*, *24*(2), 221–231.

Charlton, R., Barrick, T., Lawes, I., Markus, H., & Morris, R. (2010). White matter pathways associated with working memory in normal aging. *Cortex*, *46*(4), 474–489.

Chen, T., Chen, Y., Cheng, T., Hua, M., Liu, H., & Chiu, M. (2009). Executive dysfunction and periventricular diffusion tensor changes in amnesic mild cognitive impairment and early Alzheimer's disease. *Human Brain Mapping*, *30*(11), 3826–3836.

Chenevert, T., Brunberg, J., & Pipe, J. (1990). Anisotropic diffusion in human white matter: demonstration with MR techniques in vivo. *Radiology*, *177*(2), 401–405.

Clark, R., Hutton, M., Fuldner, M., Froelich, S., Karran, E., Talbot, C., et al. (1995). The structure of the presenilin 1 (S182) gene and identification of six novel mutations in early onset AD families. *Nature Genetics*, *11*(2), 219–222.

Concha, L., Gross, D., Wheatley, B., & Beaulieu, C. (2006). Diffusion tensor imaging of time-dependent axonal and myelin degradation after corpus callosotomy in epilepsy patients. *NeuroImage*, *32*(3), 1090–1099.

Conturo, T., Lori, N., Cull, T., Akbudak, E., Snyder, A., Shimony, J., et al. (1999). Tracking neuronal fiber pathways in the living human brain. *Proceedings of the National Academy of Sciences*, *96*(18), 10422–10427.

Damoiseaux, J., Smith, S., Witter, M., Sanz-Arigita, E., Barkhof, F., Scheltens, P., et al. (2009). White matter tract integrity in aging and Alzheimer's disease. *Human Brain Mapping*, *30*(4), 1051–1059.

Davis, S., Dennis, N., Buchler, N., White, L., Madden, D., & Cabeza, R. (2009). Assessing the effects of age on long white matter tracts using diffusion tensor tractography. *NeuroImage*, *46*(2), 530–541.

De Jager, C., Milwain, E., & Budge, M. (2002). Early detection of isolated memory deficits in the elderly: the need for more sensitive neuropsychological tests. *Psychological Medicine*, *32*(3), 483–491.

de Zubicaray, G. I., Rose, S. E., & McMahon, K. L. (2011). The structure and connectivity of semantic memory in the healthy older adult brain. *NeuroImage*, *54*, 1488–1494.

Douaud, G., Jbabdi, S., Behrens, T. E. J., Menke, R. A., Gass, A., Monsh, A. U., et al. (2011). DTI measures in crossing-fibre areas: Increased diffusion anisotropy reveals early white matter alteration in MCI and mild Alzheimer's disease. *NeuroImage*, *55*, 880–890.

Duan, J., Wang, H., Xu, J., Lin, X., Chen, S., Kang, Z., et al. (2006). White matter damage of patients with Alzheimer's disease correlated with the decreased cognitive

function. *Surgical and Radiologic Anatomy*, *28*(2), 150–156.

Dvorine, I. (1963). Quantitative classification of color blind. *The Journal of General Psychology*, *68*, 255–65.

Ecker, U., Zimmer, H., & Groh-Bordin, C. (2007). Color and context: An ERP study on intrinsic and extrinsic feature binding in episodic memory. *Memory & Cognition*, *35*(6), 1483–1501.

Fellgiebel, A., Wille, P., Müller, M., Winterer, G., Scheurich, A., Vucurevic, G., et al. (2004). Ultrastructural hippocampal and white matter alterations in mild cognitive impairment: a diffusion tensor imaging study. *Dementia and Geriatric Cognitive Disorders*, *18*(1), 101–108.

Folstein, M., Folstein, S., & McHugh, P. (1975). Mini-Mental State: a practical method for grading the cognitive state of patients for the clinician. *Journal of Psychiatric Research*, *12*(3), 189–98.

Frisoni, G., Pievani, M., Testa, C., Sabattoli, F., Bresciani, L., Bonetti, M., et al. (2007). The topography of grey matter involvement in early and late onset Alzheimer's disease. *Brain*, *130*(3), 720–730.

Frye, R., Liederman, J., Hasan, K., Lincoln, A., Malmberg, B., McLean III, J., et al. (2010). Diffusion tensor quantification of the relations between microstructural and macrostructural indices of white matter and reading. *Human Brain Mapping*, *32*, 1220–1235.

Gallo, D., Sullivan, A., Daffner, K., Schacter, D., & Budson, A. (2004). Associative recognition in Alzheimer's disease: evidence for impaired recall-to-reject. *Neuropsychology*, *18*(3), 556–563.

Gelman, A., Su, Y.-S., Yajima, M., & Hill, J. (2011). arm: Data analysis using regression and multilevel/hierarchical models [Computer software manual]. Available from `http://CRAN.R-project.org/package=arm` (R package version 1.4-07)

Goate, A., Chartier-Harlin, M., Mullan, M., Brown, J., Crawford, F., Fidani, L., et al. (1991). Segregation of a missense mutation in the amyloid precursor protein gene with familial Alzheimer's disease. *Nature*, *349*(6311), 704–706.

Goldman, J., Hahn, S., Catania, J., LaRusse-Eckert, S., Butson, M., Rumbaugh, M., et al. (2011). Genetic counseling and testing for Alzheimer disease: Joint practice guidelines of the American College of Medical Genetics and the National Society of Genetic Counselors. *Genetics in Medicine*, *13*(6), 597–605.

Good, C., Johnsrude, I., Ashburner, J., Henson, R., Friston, K., & Frackowiak, R. (2001). A voxel-based morphometric study of ageing in 465 normal adult human brains. *NeuroImage*, *14*(1), 21–36.

Gulani, V., & Sundgren, P. (2006). Diffusion tensor magnetic resonance imaging. *Journal of Neuro-ophthalmology*, *26*(1), 51–60.

Hardy, J. (1997). Amyloid, the presenilins and Alzheimer's . *Trends in Neurosciences*, *20*(4), 154–159.

Hasan, K., Iftikhar, A., Kamali, A., Kramer, L., Ashtari, M., Cirino, P., et al. (2009). Development and aging of the healthy human brain uncinate fasciculus across the lifespan using diffusion tensor tractography. *Brain Research*, *1276*, 67–76.

Head, D., Buckner, R., Shimony, J., Williams, L., Akbudak, E., Conturo, T., et al. (2004). Differential vulnerability of anterior white matter in nondemented aging with minimal acceleration in dementia of the Alzheimer type: evidence from diffusion tensor imaging. *Cerebral Cortex*, *14*(4), 410–423.

Holmes, C. (2002). Genotype and phenotype in Alzheimer's disease. *The British Journal of Psychiatry*, *180*(2), 131–134.

Horsfield, M., & Jones, D. (2002). Applications of diffusion-weighted and diffusion tensor MRI to white matter diseases–a review. *NMR in Biomedicine*, *15*(7-8), 570–577.

Jeneson, A., Mauldin, K., & Squire, L. (2010). Intact working memory for relational information after medial temporal lobe damage. *Journal of Neuroscience*, *30*(41), 13624–13629.

Jenkinson, M., & Smith, S. (2001). A global optimisation method for robust affine registration of brain images. *Medical Image Analysis*, *5*(2), 143–156.

Jonides, J., Smith, E., Koeppe, R., Awh, E., Minoshima, S., & Mintun, M. (1993). Spatial working-memory in humans as revealed by PET. *Nature*, *363*(6430), 623–625.

Kahneman, D., Treisman, A., & Gibbs, B. (1992). The reviewing of object files: Object-specific integration of information. *Cognitive Psychology*, *24*(2), 175–219.

Kantarci, K., Petersen, R., Boeve, B., Knopman, D., Weigand, S., O'Brien, P., et al. (2005). DWI predicts future progression to Alzheimer disease in amnestic mild cognitive impairment. *Neurology*, *64*(5), 902.

Kaplan, E., Goodglass, H., & Weintraub, S. (1983). *Boston naming test (revised 60-item version)*. Philadelphia: Lea & Febiger.

Karlsen, P., Allen, R., Baddeley, A., & Hitch, G. (2010). Binding across space and time in visual working memory. *Memory & Cognition*, *38*(3), 292–303.

Kiuchi, K., Morikawa, M., Taoka, T., Nagashima, T., Yamauchi, T., Makinodan, M., et al. (2009). Abnormalities of the uncinate fasciculus and posterior cingulate fasciculus in mild cognitive impairment and early Alzheimer's disease: A diffusion tensor tractography study. *Brain Research*, *1287*, 184–191.

Kraus, M., Susmaras, T., Caughlin, B., Walker, C., Sweeney, J., & Little, D. (2007). White matter integrity and cognition in chronic traumatic brain injury: a diffusion tensor imaging study. *Brain*, *130*(10), 2508–2519.

Lavenex, P., & Amaral, D. (2000). Hippocampal-neocortical interaction: a hierarchy of associativity. *Hippocampus*, *10*(4), 420–430.

Le Bihan, D. (2003). Looking into the functional architecture of the brain with diffusion MRI. *Nature Reviews Neuroscience*, *4*(6), 469–480.

Le Bihan, D., & Breton, E. (1985). Imagerie de diffusion in vivo par résonance magnétique nucléaire. *C. R. Acad. Sci. (Paris)*, *301*, 1109–1112.

Le Bihan, D., Mangin, J., Poupon, C., Clark, C., Pappata, S., Molko, N., et al. (2001). Diffusion tensor imaging: concepts and applications. *Journal of Magnetic Resonance Imaging*, *13*(4), 534–546.

Lee, A., Rahman, S., Hodges, J., Sahakian, B., & Graham, K. (2003). Associative and recognition memory for novel objects in dementia: implications for diagnosis. *European Journal of Neuroscience*, *18*(6), 1660–1670.

Lemere, C., Lopera, F., Kosik, K., Lendon, C., Ossa, J., Saido, T., et al. (1996). The E280A presenilin 1 Alzheimer mutation produces increased A$\beta$42 deposition and severe cerebellar pathology. *Nature Medicine*, *2*(10), 1146–1150.

Lendon, C., Martinez, A., Behrens, I., Kosik, K., Madrigal, L., Norton, J., et al. (1997). E280A PS-1 mutation causes Alzheimer's disease but age of onset is not modified by ApoE alleles. *Human Mutation*, *10*(3), 186–195.

Levy-Lahad, E., Wasco, W., Poorkaj, P., Romano, D., Oshima, J., Pettingell, W., et al. (1995). Candidate gene for the chromosome 1 familial Alzheimer's disease locus. *Science*, *269*(5226), 973–977.

Lindeboom, J., Schmand, B., Tulner, L., Walstra, G., & Jonker, C. (2002). Visual association test to detect early dementia of the Alzheimer type. *Journal of Neurology, Neurosurgery & Psychiatry*, *73*(2), 126–133.

Logie, R., Cocchini, G., Delia Sala, S., & Baddeley, A. (2004). Is there a specific executive capacity for dual task coordination? Evidence from Alzheimer's disease. *Neuropsychology*, *18*(3), 504–513.

Logie, R., Della Sala, S., MacPherson, S., & Cooper, J. (2007). Dual task demands on encoding and retrieval processes: Evidence from healthy adult ageing. *Cortex*, *43*, 159–169.

Lopera, F., Ardilla, A., Martínez, A., Madrigal, L., Arango-Viana, J., Lemere, C., et al. (1997). Clinical features of early-onset Alzheimer disease in a large kindred with an E280A presenilin-1 mutation. *The Journal of the American Medical Association*, *277*(10), 793–799.

Loui, P., Li, H., & Schlaug, G. (2011). White matter integrity in right hemisphere predicts pitch-related grammar learning. *NeuroImage*, *55*(2), 500–507.

Lowndes, G., Saling, M., Ames, D., Chiu, E., Gonzalez, L., & Savage, G. (2008). Recall and recognition of verbal paired associates in early Alzheimer's disease. *Journal of the International Neuropsychological Society*, *14*(04), 591–600.

Lowndes, G., & Savage, G. (2007). Early detection of memory impairment in Alzheimer's disease: a neurocognitive perspective on assessment. *Neuropsychology Review*, *17*(3), 193–202.

Luck, S., & Vogel, E. (1997). The capacity of visual working memory for features and conjunctions. *Nature*, *390*(6657), 279–280.

Madden, D., Spaniol, J., Costello, M., Bucur, B., White, L., Cabeza, R., et al. (2009). Cerebral white matter integrity mediates adult age differences in cognitive perfor-

mance. *Journal of Cognitive Neuroscience*, *21*(2), 289–302.

Madden, D., Whiting, W., Huettel, S., White, L., MacFall, J., & Provenzale, J. (2004). Diffusion tensor imaging of adult age differences in cerebral white matter: relation to response time. *NeuroImage*, *21*(3), 1174–1181.

Mayes, A., Montaldi, D., & Migo, E. (2007). Associative memory and the medial temporal lobes. *Trends in Cognitive Sciences*, *11*(3), 126–135.

McKhann, G., Drachman, D., Folstein, M., Katzman, R., Price, D., & Stadlan, E. (1984). Clinical diagnosis of Alzheimer's disease. *Neurology*, *34*(7), 939–944.

Medina, D., Morrell, L. deToledo, Urresta, F., Gabrieli, J., Moseley, M., Fleischman, D., et al. (2006). White matter changes in mild cognitive impairment and AD: a diffusion tensor imaging study. *Neurobiology of Aging*, *27*(5), 663–672.

Meinzer, M., Mohammadi, S., Kugel, H., Schiffbauer, H., Floel, A., Albers, J., et al. (2010). Integrity of the hippocampus and surrounding white matter is correlated with language training success in aphasia. *NeuroImage*, *53*(1), 283–290.

Merboldt, K., Hanicke, W., & Frahm, J. (1985). Self-diffusion NMR imaging using stimulated echoes. *Journal of Magnetic Resonance (1969)*, *64*(3), 479–486.

Mielke, M., Kozauer, N., Chan, K., George, M., Toroney, J., Zerrate, M., et al. (2009). Regionally-specific diffusion tensor imaging in mild cognitive impairment and Alzheimer's disease. *NeuroImage*, *46*(1), 47–55.

Mori, S., & Barker, P. (1999). Diffusion magnetic resonance imaging: its principle and applications. *The Anatomical Record*, *257*(3), 102–109.

Morris, J., Heyman, A., Mohs, R., Hughes, J., et al. (1989). The consortium to establish a registry for Alzheimer's disease (CERAD): I. Clinical and neuropsychological assessment of Alzheimer's disease. *Neurology*, *39*, 1159–1165.

Moseley, M., Cohen, Y., Mintorovitch, J., Chileuitt, L., Shimizu, H., Kucharczyk, J., et al. (1990). Early detection of regional cerebral ischemia in cats: comparison of diffusion-and T2-weighted MRI and spectroscopy. *Magnetic Resonance in Medicine*, *14*(2), 330–346.

Nestor, P., Kubicki, M., Gurrera, R., Niznikiewicz, M., Frumin, M., McCarley, R., et al. (2004). Neuropsychological correlates of diffusion tensor imaging in schizophrenia. *Neuropsychology*, *18*(4), 629–637.

Oishi, K., Faria, A., Zijl, P., & Mori, S. (2011). *MRI atlas of human white matter.* New York: Academic Press.

Osterrieth, P. (1944). Le test de copie d'une figure complexe; contribution à l'étude de la perception et de la mémoire. *Archives de Psychologie*, *30*, 206–356.

O'Sullivan, M., Jones, D., Summers, P., Morris, R., Williams, S., & Markus, H. (2001). Evidence for cortical "disconnection" as a mechanism of age-related cognitive decline. *Neurology*, *57*(4), 632–638.

Pariente, J., Cole, S., Henson, R., Clare, L., Kennedy, A., Rossor, M., et al. (2005). Alzheimer's patients engage an alternative network during a memory task. *Annals*

*of Neurology*, *58*(6), 870–879.

Park, H., Kubicki, M., Shenton, M., Guimond, A., McCarley, R., Maier, S., et al. (2003). Spatial normalization of diffusion tensor MRI using multiple channels. *NeuroImage*, *20*(4), 1995–2009.

Parra, M., Abrahams, S., Fabi, K., Logie, R., Luzzi, S., & Sala, S. (2009). Short-term memory binding deficits in Alzheimer's disease. *Brain*, *132*(4), 1057–1066.

Parra, M., Abrahams, S., Logie, R., & Della Sala, S. (2010). Visual short-term memory binding in Alzheimer's disease and depression. *Journal of Neurology*, 1–10.

Parra, M., Abrahams, S., Logie, R., Mendez, L., Lopera, F., & Della Sala, S. (2010). Visual short-term memory binding deficits in familial Alzheimer's disease. *Brain*, *13*(9), 2702–2713.

Parra, M., Sala, S., Abrahams, S., Logie, R., Méndez, L., & Lopera, F. (2011). Specific deficit of colour-colour short-term memory binding in sporadic and familial Alzheimer's Disease. *Neuropsychologia*, *49*, 1943–1952.

Paulesu, E., Frith, C., & Frackowiak, R. (1993). The neural correlates of the verbal component of working memory. *Nature*, *362*, 342–345.

Persson, J., Lind, J., Larsson, A., Ingvar, M., Cruts, M., Van Broeckhoven, C., et al. (2006). Altered brain white matter integrity in healthy carriers of the APOE $\epsilon$4 allele: A risk for AD? *Neurology*, *66*(7), 1029–1033.

Petersen, R. (2004). Mild cognitive impairment as a diagnostic entity. *Journal of Internal Medicine*, *256*(3), 183–194.

Piekema, C., Kessels, R., Mars, R., Petersson, K., & Fernández, G. (2006). The right hippocampus participates in short-term memory maintenance of object-location associations. *Neuroimage*, *33*(1), 374–382.

Piekema, C., Rijpkema, M., Fernández, G., Kessels, R., & Aleman, A. (2010). Dissociating the neural correlates of intra-item and inter-item working-memory binding. *PloS ONE*, *5*(4), e10214.

Pierpaoli, C., & Basser, P. (1996). Toward a quantitative assessment of diffusion anisotropy. *Magnetic Resonance in Medicine*, *36*(6), 893–906.

Pievani, M., Agosta, F., Pagani, E., Canu, E., Sala, S., Absinta, M., et al. (2010). Assessment of white matter tract damage in mild cognitive impairment and Alzheimer's disease. *Human Brain Mapping*, *31*(12), 1862–1875.

Prabhakaran, V., Narayanan, K., Zhao, Z., & Gabrieli, J. (2000). Integration of diverse information in working memory within the frontal lobe. *Nature Neuroscience*, *3*(1), 85–90.

Querfurth, H., & LaFerla, F. (2010). Mechanisms of disease: Alzheimer's disease. *The New England Journal of Medicine*, *362*, 329–44.

Reitan, R. (1958). Validity of the Trail Making Test as an indicator of organic brain damage. *Perceptual and Motor Skills*, *8*, 271–276.

Rey, A. (1941). L'examen psychologique dans les cas d'encéphalopathie traumatique.(les

problems.). *Archives de Psychologie*, *28*, 215–285.

Ringman, J., O'Neill, J., Geschwind, D., Medina, L., Apostolova, L., Rodriguez, Y., et al. (2007). Diffusion tensor imaging in preclinical and presymptomatic carriers of familial Alzheimer's disease mutations. *Brain*(7), 1767–1776.

Rose, S., Chen, F., Chalk, J., Zelaya, F., Strugnell, W., Benson, M., et al. (2000). Loss of connectivity in Alzheimer's disease: an evaluation of white matter tract integrity with colour coded MR diffusion tensor imaging. *Journal of Neurology, Neurosurgery & Psychiatry*, *69*(4), 528–530.

Rose, S., Janke PhD, A., & Chalk, J. (2008). Gray and white matter changes in Alzheimer's disease: a diffusion tensor imaging study. *Journal of Magnetic Resonance Imaging*, *27*(1), 20–26.

Rose, S., McMahon, K., Janke, A., O'Dowd, B., de Zubicaray, G., Strudwick, M., et al. (2006). Diffusion indices on magnetic resonance imaging and neuropsychological performance in amnestic mild cognitive impairment. *Journal of Neurology, Neurosurgery & Psychiatry*, *77*(10), 1122–1128.

Ryan, L., Walther, K., Bendlin, B. B., Lue, L.-F., Walker, D. G., & Glisky, E. L. (2008). Age-related differences in white matter integrity and cognitive function are related to APOE status. *NeuroImage*, *54*, 1565–1577.

Sakuma, H., Nomura, Y., Takeda, K., Tagami, T., Nakagawa, T., Tamagawa, Y., et al. (1991). Adult and neonatal human brain: diffusional anisotropy and myelination with diffusion-weighted MR imaging. *Radiology*, *180*(1), 229–233.

Sala, J., & Courtney, S. (2007). Binding of what and where during working memory maintenance. *Cortex*, *43*, 5–21.

Salat, D., Tuch, D., Kouwe, A. Van der, Greve, D., Pappu, V., Lee, S., et al. (2010). White matter pathology isolates the hippocampal formation in Alzheimer's disease. *Neurobiology of Aging*, *31*(2), 244–256.

Saunders, A., Strittmatter, W., Schmechel, D., St George-Hyslop, P., Pericak-Vance, M., Joo, S., et al. (1993). Association of apolipoprotein E allele $\epsilon 4$ with late-onset familial and sporadic Alzheimer's disease. *Neurology*, *43*(8), 1467–1472.

Saykin, A., Shen, L., Foroud, T., Potkin, S., Swaminathan, S., Kim, S., et al. (2010). Alzheimer's Disease Neuroimaging Initiative biomarkers as quantitative phenotypes: Genetics core aims, progress, and plans. *Alzheimer's and Dementia*, *6*(3), 265–273.

Scholz, J., Klein, M., Behrens, T., & Johansen-Berg, H. (2009). Training induces changes in white-matter architecture. *Nature Neuroscience*, *12*(11), 1370–1371.

Sherrington, R., Rogaev, E., Liang, Y., Rogaeva, E., Levesque, G., Ikeda, M., et al. (1995). Cloning of a gene bearing missense mutations in early-onset familial Alzheimer's disease. *Nature*, *375*(6534), 754–760.

Simon, T., Ding, L., Bish, J., McDonald-McGinn, D., Zackai, E., & Gee, J. (2005). Volumetric, connective, and morphologic changes in the brains of children with chromosome 22q11. 2 deletion syndrome: an integrative study. *NeuroImage*, *25*(1),

169–180.

Small, D., & McLean, C. (1999). Alzheimer's disease and the amyloid $\beta$ protein. *Journal of Neurochemistry*, *73*(2), 443–449.

Small, G., Rabins, P., Barry, P., Buckholtz, N., DeKosky, S., Ferris, S., et al. (1997). Diagnosis and treatment of alzheimer disease and related disorders. *The Journal of the American Medical Association*, *278*(16), 1363.

Smith, E., & Jonides, J. (1997). Working memory: A view from neuroimaging. *Cognitive Psychology*, *33*, 5–42.

Smith, S., Jenkinson, M., Johansen-Berg, H., Rueckert, D., Nichols, T., Mackay, C., et al. (2006). Tract-based spatial statistics: voxelwise analysis of multi-subject diffusion data. *NeuroImage*, *31*(4), 1487–1505.

Smith, S., Johansen-Berg, H., Jenkinson, M., Rueckert, D., Nichols, T., Miller, K., et al. (2007). Acquisition and voxelwise analysis of multi-subject diffusion data with tract-based spatial statistics. *Nature Protocols*, *2*(3), 499–503.

Sperling, R., Bates, J., Chua, E., Cocchiarella, A., Rentz, D., Rosen, B., et al. (2003). fMRI studies of associative encoding in young and elderly controls and mild Alzheimer's disease. *Journal of Neurology, Neurosurgery & Psychiatry*, *74*(1), 44–50.

Stejskal, E., & Tanner, J. (1965). Spin diffusion measurements: spin echoes in the presence of a time-dependent field gradient. *The Journal of Chemical Physics*, *42*(1), 288–292.

Stricker, N., Schweinsburg, B., Delano-Wood, L., Wierenga, C., Bangen, K., Haaland, K., et al. (2009). Decreased white matter integrity in late-myelinating fiber pathways in Alzheimer's disease supports retrogenesis. *NeuroImage*, *45*(1), 10–16.

Strittmatter, W., Saunders, A., Schmechel, D., Pericak-Vance, M., Enghild, J., Salvesen, G., et al. (1993). Apolipoprotein E: high-avidity binding to beta-amyloid and increased frequency of type 4 allele in late-onset familial Alzheimer disease. *Proceedings of the National Academy of Sciences*, *90*(5), 1977–1981.

Sullivan, E., Adalsteinsson, E., Hedehus, M., Ju, C., Moseley, M., Lim, K., et al. (2001). Equivalent disruption of regional white matter microstructure in ageing healthy men and women. *Neuroreport*, *12*(1), 99–104.

Sumerall, S., Timmons, P., James, A., Ewing, M., & Oehlert, M. (1997). Expanded norms for the controlled oral word association test. *Journal of Clinical Psychology*, *53*(5), 517–521.

Swainson, R., Hodges, J., Galton, C., Semple, J., Michael, A., Dunn, B., et al. (2000). Early detection and differential diagnosis of Alzheimer's disease and depression with neuropsychological tasks. *Dementia and Geriatric Cognitive Disorders*, *12*(4), 265–280.

Taylor, D., & Bushell, M. (1985). The spatial mapping of translational diffusion coefficients by the NMR imaging technique. *Physics in Medicine and Biology*, *30*,

345–349.

Tench, C., Morgan, P., Wilson, M., & Blumhardt, L. (2002). White matter mapping using diffusion tensor MRI. *Magnetic Resonance in Medicine*, *47*(5), 967–972.

Todd, J., & Marois, R. (2005). Posterior parietal cortex activity predicts individual differences in visual short-term memory capacity. *Cognitive, Affective, & Behavioral Neuroscience*, *5*(2), 144.

Treisman, A. (1996). The binding problem. *Current Opinion in Neurobiology*, *6*(2), 171–178.

Uncapher, M., Otten, L., & Rugg, M. (2006). Episodic encoding is more than the sum of its parts: An fMRI investigation of multifeatural contextual encoding. *Neuron*, *52*(3), 547–556.

van Essen, D., Anderson, C., & Felleman, D. (1992). Information processing in the primate visual system: an integrated systems perspective. *Science*, *255*(5043), 419–423.

Vogel, E., Woodman, G., & Luck, S. (2001). Storage of features, conjunctions, and objects in visual working memory. *Journal of Experimental Psychology: Human Perception and Performance*, *27*(1), 92–114.

Wechsler, D. (1945). A standardized memory scale for clinical use. *Journal of Psychology: Interdisciplinary and Applied*, *19*, 87–95.

Wimberger, D., Roberts, T., Barkovich, A., Prayer, L., Moseley, M., & Kucharczyk, J. (1995). Identification of "premyelination" by diffusion-weighted mri. *Journal of Computer Assisted Romography*, *19*(1), 28–33.

Wimo, A., & Prince, M. (2010). World Alzheimer Report 2010 - The Global Economic Impact of Dementia. *Alzheimer's Disease International*.

Xie, S., Xiao, J., Gong, G., Zang, Y., Wang, Y., Wu, H., et al. (2006). Voxel-based detection of white matter abnormalities in mild Alzheimer disease. *Neurology*, *66*(12), 1845–1849.

Ystad, M., Hodneland, E., Adolfsdottir, S., Haász, J., Lundervold, A., Eichele, T., et al. (2011). Cortico-striatal connectivity and cognition in normal aging: A combined DTI and resting state fMRI study. *NeuroImage*, *55*(1), 24–31.

Zhang, Y., Schuff, N., Jahng, G., Bayne, W., Mori, S., Schad, L., et al. (2007). Diffusion tensor imaging of cingulum fibers in mild cognitive impairment and Alzheimer disease. *Neurology*, *68*(1), 13–19.

Zhuang, L., Wen, W., Zhu, W., Trollor, J., Kochan, N., Crawford, J., et al. (2010). White matter integrity in mild cognitive impairment: a tract-based spatial statistics study. *NeuroImage*, *53*(1), 16–25.

Zimmer, H., Mecklinger, A., & Lindenberger, U. (2006). Levels of binding: Types, mechanisms, and functions of binding in remembering. In H. Zimmer, A. Mecklinger, & U. Lindenberger (Eds.), *Handbook of binding and memory: Perspectives from cognitive neuroscience* (pp. 3–24). New York: Oxford University Press.

# A List of abbreviations

| | |
|---|---|
| AD | Alzheimer' disease |
| FAD | familial Alzheimer's disease |
| SAD | sporadic Alzheimer's disease |
| AC | asymptomatic carrier |
| HC | healthy control |
| | |
| DTI | diffusion tensor imaging |
| DI | diffusion imaging |
| MRI | magnetic resonance imaging |
| fMRI | functional magnetic resonance imaging |
| MNI | Montreal Neurological Institute |
| ROI | region of interest |
| FA | fractional anisotropy |
| $\overline{D}$ | mean diffusivity |
| | |
| STM | short-term memory |
| LTM | long-term memory |
| PAL | paired-associates learning task |
| MMSE | Mini-Mental Status Examination |
| | |
| DL-PFC | dorsolateral prefrontal cortex |
| A-PFC | anterior prefrontal cortex |
| BR-PFC | Broca's area and corresponding in right hemisphere |
| SLF | superior longitudinal fasciculus |
| ILF | inferior longitudinal fasciculus |
| IFO | inferior fronto-occipital fasciculus |
| UNC | uncinate fasciculus |
| CGC | cingulate gyrus part of cingulum |
| CGH | hippocampal part of cingulum |
| FX | fornix |
| ATR | anterior thalamic radiations |
| CST | corticospinal tract |
| GCC | genu of corpus callosum |
| SCC | splenium of corpus callosum |
| CS | centrum semiovale |
| F-WM | frontal white matter |
| P-WM | parietal white matter |
| T-WM | temporal white matter |

# B MNI coordinates of regions of interest

Table 12: MNI coordinates for regions of interest.

| | | MNI coordinates | | | | | |
|---|---|---|---|---|---|---|---|
| ROI | Side | x, y, z | x, y, z | x, y, z | x, y, z | x, y, z | x, y, z |
| DL-PFC | left | -30, 34, 23 | -33, 37, 20 | -31, 39, 17 | | | |
| | right | 30, 31, 23 | 34, 37, 20 | 32, 39, 17 | | | |
| A-PFC | left | -12, 45, 35 | -12, 48, 39 | -13, 50, 25 | | | |
| | right | 12, 45, 35 | 12, 48, 30 | 13, 50, 25 | | | |
| BR-PFC | left | -37, 15, 20 | -37, 20, 15 | -43, 11, 10 | | | |
| | right | 37, 15, 20 | 37, 20, 15 | 45, 12, 10 | | | |
| SLF | left | -33, -40, 30 | -38, -30, 30 | -38, -20, 30 | | | |
| | right | 33, -40, 30 | 38, -30, 30 | 38, -20, 30 | | | |
| IFO | left | -32, 0, -7 | -33, -7, -7 | -34, -16, -7 | | | |
| | right | 32, 0, -7 | 33, -7, -7 | 36, -15, -7 | | | |
| ILF | left | -43, -20, -10 | -43, -30, -10 | -43, -40, -10 | | | |
| | right | 43, -20, -10 | 44, -30, -10 | 43, -40, -10 | | | |
| UNC | left | -24, 15, -11 | -27, 9, -11 | -34, 1, -11 | | | |
| | right | 25, 15, -11 | 30, 9, -11 | 33, 4, -11 | | | |
| CGC | left | -7, 0, 35 | -7, -10, 35 | -7, -20, 35 | | | |
| | right | 8, 0, 35 | 8, -10, 35 | 8, -20, 35 | | | |
| CGH | left | -21, -34, -12 | -21, -28, -17 | -24, -24, -22 | | | |
| | right | 24, -31, -12 | 23, -26, -17 | 24, -22, -22 | | | |
| FX | middle | 0, 1, 7 | | | | | |
| ATR | left | -21, 25, 10 | -22, 19, 10 | -17, 7, 10 | -13, 0, 10 | | |
| | right | 21, 25, 10 | 22, 19, 10 | 17, 7, 10 | 17, 7, 10 | | |
| CST | left | -22, 18, 17 | -22, -18, 12 | -22, -18, 7 | | | |
| | right | 22, -18, 17 | 22, -18, 12 | 22, -18, 7 | | | |
| GCC | left | -10, 29, 10 | -8, 30, 3 | | | | |
| | middle | 0, 26, 10 | 0, 26, 3 | | | | |
| | right | 10, 30, 10 | 9, 30, 3 | | | | |
| SCC | left | -12, -44, 12 | -10, -41, 19 | | | | |
| | middle | 0, -38, 12 | 0, -36, 19 | | | | |
| | right | 15, -44, 12 | 12, -41, 19 | | | | |
| CS | left | -22, 10, 36 | -24, 0, 36 | -26, -10, 36 | -28, -20, 36 | -26, -30, 36 | -24, -40, 36 |
| | right | 22, 10, 36 | 24, 0, 36 | 26, -10, 36 | 28, -20, 36 | 26, -30, 36 | 24, -40, 36 |
| F-WM | left | -19, 37, 1 | -26, 37, 1 | -23, 44, 1 | -19, 35, 8 | -26, 35, 8 | -21, 42, 8 |
| | right | 20, 37, 1 | 27, 37, 1 | 24, 44, 1 | 20, 35, 8 | 27, 35, 8 | 24, 42, 8 |
| P-WM | left | -25, 56, 40 | -18, -62, 40 | -20, -53, 40 | -17, -60, 45 | -18, -55, 45 | -20, -50, 45 |
| | right | 25, -56, 40 | 18, -62, 40 | 20, -53, 40 | 17, -60, 45 | 18, -55, 45 | 20, -50, 45 |
| T-WM | left | -41, -3, -22 | -46, -10, -22 | -40, 1, -29 | -33, 1, -29 | -47, -16, -19 | -42, -9, -19 |
| | right | 41, -3, -22 | 46, -10, -22 | 40, 1, -29 | 33, 1, -29 | 46, -16, -19 | 42, -9, -19 |

# C Supplementary results

Table 13: Comparisons of FA and $\overline{D}$ values between hemispheres.

| | FA values | | | $\overline{D}$ values | | |
|---|---|---|---|---|---|---|
| ROI | $t$ test (df) | $p$ value | direction of differences | $t$ test (df) | $p$ value | direction of differences |
| DL-PFC | -2.41 (345) | .017 | higher in right | 1.31 (345) | ns | |
| A-PFC | -3.76 (322) | <.001 | higher in right | -0.20 (346) | ns | |
| BR-PFC | 12.19 (294) | <.001 | higher in left | 4.45 (345) | <.001 | lower in right |
| SLF | -4.30 (329) | <.001 | higher in right | 6.39 (322) | <.001 | lower in right |
| ILF | -2.24 (346) | .026 | higher in right | 6.27 (344) | <.001 | lower in right |
| IFO | -0.93 (336) | ns | | 5.25 (346) | <.001 | lower in right |
| UNC | -5.74 (346) | <.001 | higher in right | 3.29 (345) | .001 | lower in right |
| CGH | 6.41 (343) | <.001 | higher in left | 7.55 (344) | <.001 | lower in right |
| CGC | 1.57 (344) | ns | | 2.24 (346) | .026 | lower in right |
| ATR | 1.11 (461) | ns | | 3.04 (462) | .003 | lower in right |
| CST | 4.26 (330) | <.001 | higher in left | 5.19 (337) | <.001 | lower in right |
| GCC | 8.74 (230) | <.001 | higher in left | -2.76 (219) | .006 | lower in left |
| SCC | -8.43 (192) | <.001 | higher in right | 0.87 (230) | ns | |
| CS | -5.36 (645) | <.001 | higher in right | 8.86 (619) | <.001 | lower in right |
| F-WM | 2.32 (694) | .021 | higher in left | -6.59 (694) | <.001 | lower in left |
| P-WM | -3.04 (644) | .002 | higher in right | -0.22 (678) | ns | |
| T-WM | -0.57 (685) | ns | | 8.53 (655) | <.001 | |

Table 14: Correlations between behavioural variables in control group.

| | 1. | 2. | 3. | 4. | 5. | 6. | 7. | 8. | 9. | 10. | 11. | 12. | 13. | 14. | 15. | 16. | 17. | 18. | 19. | 20. |
|---|---|---|---|---|---|---|---|---|---|---|---|---|---|---|---|---|---|---|---|---|
| 1. Age | | | | | | | | | | | | | | | | | | | | |
| 2. Education | -.16 | | | | | | | | | | | | | | | | | | | |
| 3. Shape only | -.24 | -.02 | | | | | | | | | | | | | | | | | | |
| 4. Colour only (1) | .33 | .16 | .06 | | | | | | | | | | | | | | | | | |
| 5. Colour only (2) | .02 | -.15 | .51 * | .56 ** | | | | | | | | | | | | | | | | |
| 6. Unbound colours | -.45* | .24 | .22 | -.23 | .07 | | | | | | | | | | | | | | | |
| 7. Colour-colour binding | -.14 | .40 | .51 * | .36 | .37 | -.07 | | | | | | | | | | | | | | |
| 8. Shape-colour binding | .19 | .26 | -.05 | .34 | .25 | -.27 | .46 * | | | | | | | | | | | | | |
| 9. PAL | .06 | .30 | .07 | .24 | -.28 | -.07 | .14 | .03 | | | | | | | | | | | | |
| 10. MMSE | -.22 | .04 | .49 | -.30 | .00 | .38 | .09 | -.30 | -.01 | | | | | | | | | | | |
| 11. Rey copy | -.30 | -.24 | -.19 | -.25 | -.06 | .02 | -.40 | .05 | -.12 | -.29 | | | | | | | | | | |
| 12. Rey recall | -.27 | .13 | .02 | -.14 | .12 | .50 * | .11 | .36 | -.11 | -.05 | -.02 | | | | | | | | | |
| 13. Letter fluency | .22 | .05 | .22 | .21 | .05 | -.03 | .23 | .07 | .21 | .00 | -.15 | .13 | | | | | | | | |
| 14. Animal fluency | .33 | .18 | -.21 | .33 | .10 | -.11 | .23 | .43 | .08 | .04 | -.21 | .16 | .53 * | | | | | | | |
| 15. Boston naming | .24 | .53 * | .12 | .39 | .17 | -.09 | .36 | .66 | .43 | .03 | -.06 | .06 | .22 | .51 * | | | | | | |
| 16. Word list immediate | -.12 | -.01 | -.28 | -.20 | -.29 | .23 | -.20 | -.34 | -.12 | .29 | -.20 | -.12 | .09 | .24 | -.04 | | | | | |
| 17. Word list delayed | .14 | .10 | -.24 | .10 | -.22 | .30 | -.07 | -.13 | .12 | .12 | -.10 | -.21 | .17 | .29 | .19 | .67 *** | | | | |
| 18. Word list recognition | -.09 | .05 | -.16 | .08 | -.20 | .22 | -.28 | -.19 | .39 | .02 | .00 | .11 | .05 | .03 | .10 | .33 | .20 | | | |
| 19. Trail Making part A | .27 | -.23 | -.07 | -.18 | -.02 | .18 | -.53 * | -.32 | -.36 | .10 | .12 | -.22 | -.24 | -.22 | -.19 | .03 | .02 | .08 | | |
| 20. WCST categories | .06 | .23 | -.04 | .11 | .30 | -.04 | .50 * | .56 ** | -.15 | -.03 | -.17 | .31 | .00 | .35 | .21 | -.10 | -.13 | -.50 * | -.40 | |
| 21. WCST TC | -.06 | -.22 | .01 | -.04 | -.10 | .12 | -.36 | -.37 | .01 | -.31 | .05 | .05 | .05 | -.28 | -.25 | .01 | .05 | .30 | .26 | -.67 *** |

*** $p < .001$, ** $p < .01$, * $p < .05$

Table 15: Correlations between behavioural variables in asymptomatic carrier group.

| | 1. | 2. | 3. | 4. | 5. | 6. | 7. | 8. | 9. | 10. | 11. | 12. | 13. | 14. | 15. | 16. | 17. | 18. | 19. | 20. |
|---|---|---|---|---|---|---|---|---|---|---|---|---|---|---|---|---|---|---|---|---|
| 1. Age | | | | | | | | | | | | | | | | | | | | |
| 2. Education | -.17 | | | | | | | | | | | | | | | | | | | |
| 3. Shape only | -.29 | -.56* | | | | | | | | | | | | | | | | | | |
| 4. Colour only (1) | -.38 | .09 | .037 | | | | | | | | | | | | | | | | | |
| 5. Colour only (2) | -.29 | -.15 | .62** | .73*** | | | | | | | | | | | | | | | | |
| 6. Unbound colours | -.11 | -.13 | .15 | .14 | .25 | | | | | | | | | | | | | | | |
| 7. Colour-colour binding | -.21 | .36 | .70*** | .37 | .65*** | .02 | | | | | | | | | | | | | | |
| 8. Shape-colour binding | -.34 | .29 | .61** | .39 | .63** | .45 | .76*** | | | | | | | | | | | | | |
| 9. PAL | -.48 | .31 | .69*** | .39 | .63** | .50* | .69*** | .75*** | | | | | | | | | | | | |
| 10. MMSE | -.25 | -.11 | .26 | .71*** | .53* | -.04 | .49* | .42 | .43 | | | | | | | | | | | |
| 11. Rey copy | -.13 | .25 | -.04 | .13 | .00 | .05 | .13 | .40 | .04 | .01 | | | | | | | | | | |
| 12. Rey recall | -.09 | .50 | .53 | .16 | .45 | -.26 | .63** | .46 | .33 | .10 | .40 | | | | | | | | | |
| 13. Letter fluency | .06 | .19 | .38 | .11 | .29 | .41 | .42 | .33 | .35 | -.06 | .26 | .43 | | | | | | | | |
| 14. Animal fluency | -.09 | .40 | .39 | .17 | .24 | .08 | .49 | .27 | .42 | .08 | .10 | .51 | .70*** | | | | | | | |
| 15. Boston naming | -.37 | .16 | .03 | .28 | .07 | .24 | .25 | .26 | .39 | .39 | .27 | .09 | .17 | .07 | | | | | | |
| 16. Word list immediate | .12 | .31 | .64*** | .30 | .41 | -.03 | .30 | .09 | .23 | .02 | -.12 | .30 | .23 | .13 | -.25 | | | | | |
| 17. Word list delayed | -.21 | .34 | .75*** | .44 | .50* | -.11 | .62** | .40 | .49 * | .26 | .13 | .54* | .30 | .40 | .04 | .69*** | | | | |
| 18. Word list recognition | -.36 | .23 | .41 | .58** | .46 | -.17 | .20 | -.08 | .37 | -.49* | -.19 | .13 | .04 | .22 | .25 | .38 | .46 | | | |
| 19. Trail Making part A | .41 | -.40 | -.60* | -.61* | -.42 | .03 | -.40 | -.15 | -.43 | -.42 | -.09 | -.18 | -.45 | -.44 | -.17 | -.61* | -.63** | -.79*** | | |
| 20. WCST categories | -.03 | .50* | .55* | .16 | .16 | .36 | .26 | .22 | .50* | .02 | -.08 | .18 | .44 | .52* | .21 | .31 | .28 | .39 | -.52* | |
| 21. WCST TC | .09 | -.03 | -.10 | .25 | .28 | -.55* | .34 | .01 | -.23 | .25 | .05 | .29 | -.13 | -.06 | -.04 | .11 | .11 | -.04 | .01 | -.57* |

*** $p < .001$, ** $p < .01$, * $p < .05$

Table 16: Correlations between behavioural variables in FAD patient group.

| | 1. | 2. | 3. | 4. | 5. | 6. | 7. | 8. | 9. | 10. | 11. | 12. | 13. | 14. | 15. | 16. | 17. | 18. | 19. | 20. |
|---|---|---|---|---|---|---|---|---|---|---|---|---|---|---|---|---|---|---|---|---|
| 1. Age | | | | | | | | | | | | | | | | | | | | |
| 2. Education | -.09 | | | | | | | | | | | | | | | | | | | |
| 3. Shape only | -.29 | -.32 | | | | | | | | | | | | | | | | | | |
| 4. Colour only (1) | -.25 | .15 | .46 | | | | | | | | | | | | | | | | | |
| 5. Colour only (2) | -.41 | -.14 | .38 | .81*** | | | | | | | | | | | | | | | | |
| 6. Unbound colours | -.57* | .37 | .38 | .69* | .69* | | | | | | | | | | | | | | | |
| 7. Colour-colour binding | -.33 | -.13 | .66* | .57 | .71** | .47 | | | | | | | | | | | | | | |
| 8. Shape-colour binding | -.59 | -.06 | .80*** | .48 | .45 | .46 | .73** | | | | | | | | | | | | | |
| 9. PAL | -.59* | .05 | .56 | .59* | .42 | .49 | .44 | .55 | | | | | | | | | | | | |
| 10. MMSE | -.10 | .10 | .60* | .52* | .45 | .11 | .66* | .47 | .69*** | | | | | | | | | | | |
| 11. Rey copy | -.17 | 42 | .31 | .69*** | .29 | .16 | .43 | .57 | .58* | .73*** | | | | | | | | | | |
| 12. Rey recall | .61** | .00 | .09 | .31 | .00 | -.33 | -.02 | -.28 | .28 | .58* | .37 | | | | | | | | | |
| 13. Letter fluency | .18 | .-.01 | .07 | .51 | .44 | .03 | .34 | -.07 | .46 | .57* | .58* | .43 | | | | | | | | |
| 14. Animal fluency | .32 | .16 | -.05 | .49 | .03 | -.44 | .02 | -.22 | .27 | .62** | .60** | .74*** | .65*** | | | | | | | |
| 15. Boston naming | .53* | .15 | -.36 | .13 | -.44 | -.54 | -.43 | -.34 | -.49 | -.17 | .26 | .34 | .08 | .28 | | | | | | |
| 16. Word list immediate | .04 | -.29 | .16 | .49 | .16 | -.33 | -.08 | -.02 | .32 | .56 | .49* | .54* | .52* | .72*** | .22 | | | | | |
| 17. Word list delayed | .28 | -.35 | -.09 | .25 | -.09 | -.53 | -.22 | -.27 | .13 | .42 | .42 | .63** | .53* | .64*** | .41 | .86 *** | | | | |
| 18. Word list recognition | -.02 | -.24 | .15 | .43 | .57 | -.08 | .38 | .01 | .23 | .58* | .28 | .58* | .40 | .60** | -.05 | .65*** | .62** | | | |
| 19. Trail Making part A | .41 | -.32 | -.37 | -.73*** | -.56 | -.33 | -.78** | -.67* | -.53* | -.75*** | -.80*** | -.47 | -.64** | -.66** | -.11 | -.62* | -.49 | -.36 | | |
| 20. WCST categories | .36 | -.33 | .45 | .38 | .10 | -.63 | .28 | .00 | .30 | .73*** | .38 | .73*** | .54* | .62* | .14 | .71*** | .60* | .66* | -.55 | |
| 21. WCST TC | -.25 | .20 | .16 | .29 | .13 | .51 | .01 | .12 | .37 | .17 | -.04 | -.06 | -.48 | -.17 | -.30 | -.10 | -.27 | .01 | -.14 | -.21 |

*** $p < .001$, ** $p < .01$, * $p < .05$